

8. Energy measurement in calorimeters

8.1 Concept of a calorimeter in particle physics

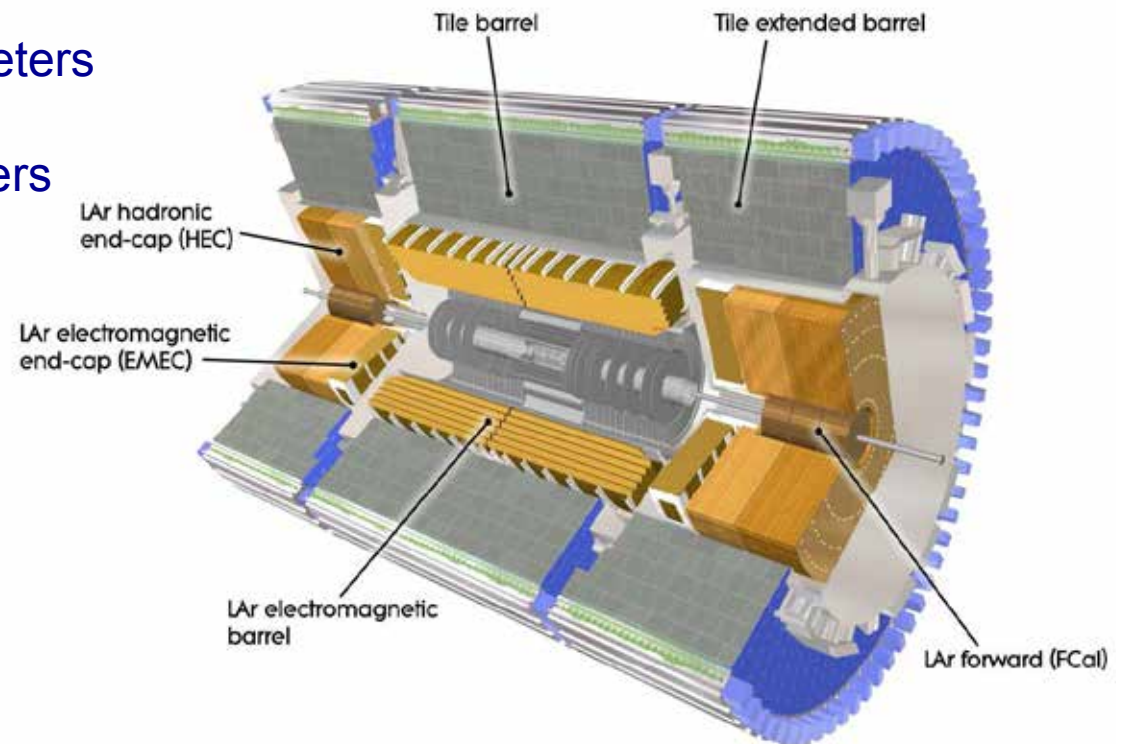
8.2 Electromagnetic calorimeter showers

8.3 Hadronic calorimeter showers

8.4 Layout and readout of calorimeters

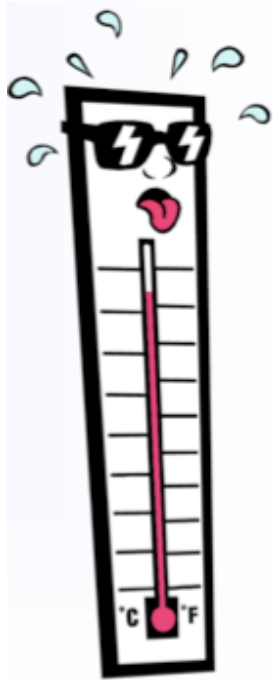
8.5 Energy resolution in calorimeters

8.6 The ATLAS and CMS calorimeter systems



Calorimetry: = Energy measurement by total absorption,
usually combined with spatial information / reconstruction

latin: calor = heat



However: calorimetry in particle physics does not correspond to measurements of ΔT

- The temperature change of 1 liter water at 20 °C by the energy deposition of a 1 GeV particle is $3.8 \cdot 10^{-14}$ K !

- LHC: total stored beam energy
 $E = 10^{14}$ protons \cdot 14 TeV $\sim 10^8$ J

If transferred to heat, this energy would only suffice to heat a mass of 239 kg water from 0° to 100°C

$$[c_{\text{Water}} = 4.18 \text{ J g}^{-1} \text{ K}^{-1}, \quad m = \Delta E / (c_{\text{Water}} \Delta T)]$$

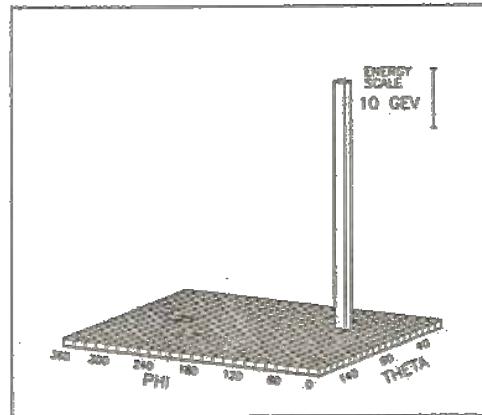
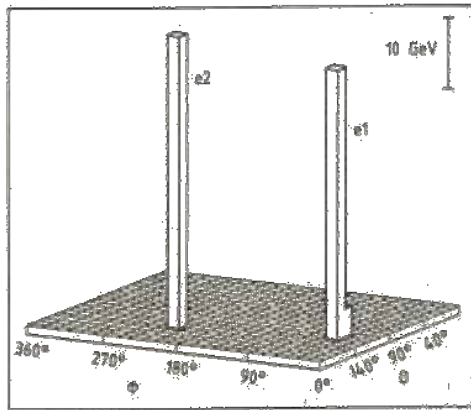
8.1 Concept of a calorimeter in particle physics

- Primary task: measurement of the total **energy of particles** via total absorption

In addition: most calorimeters are **position sensitive**, i.e. segmented, to measure

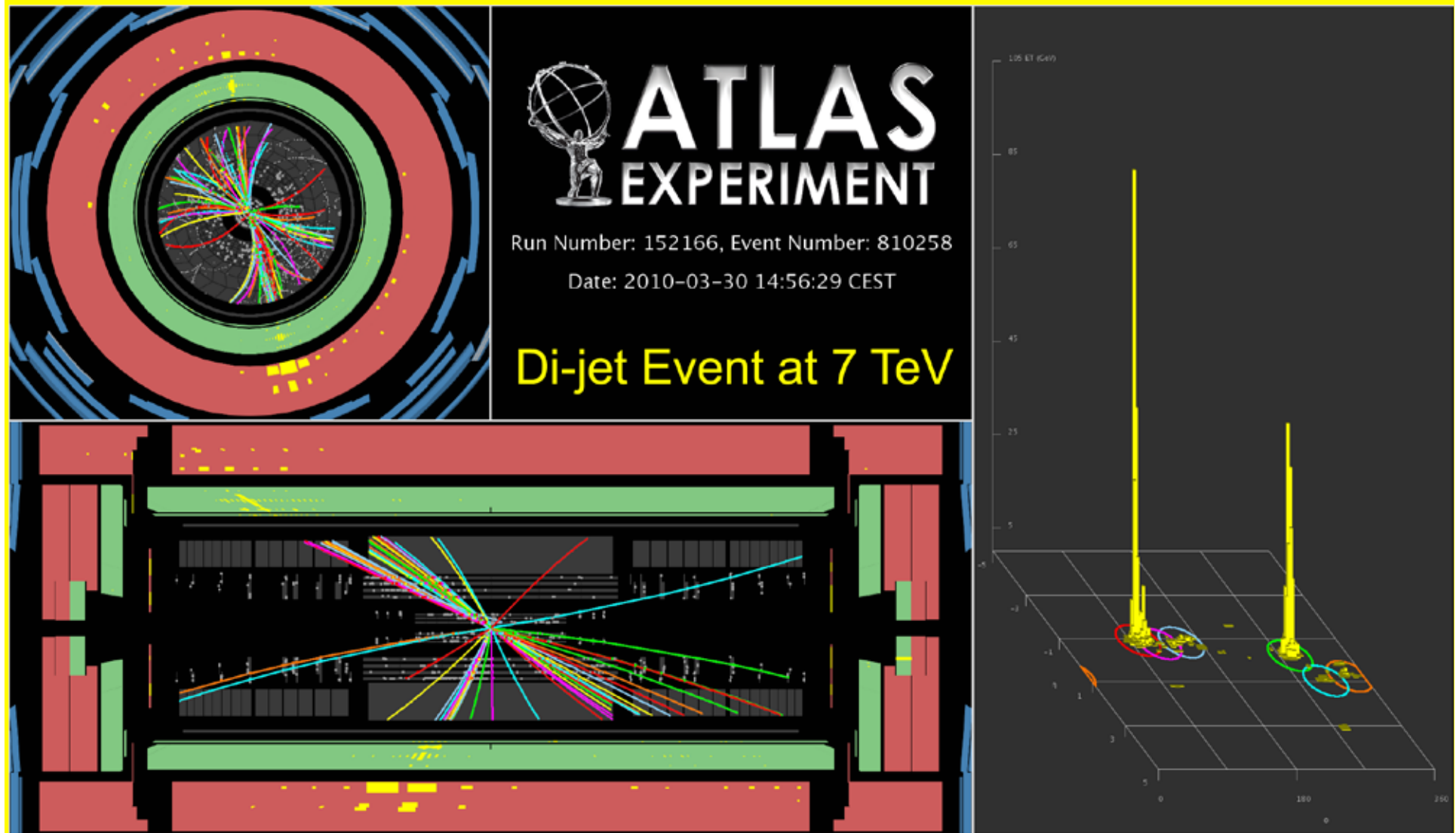
- (i) The position of the energy deposition (cell structure, η - ϕ position)
- (ii) The direction of the incoming particle (requires in addition longitudinal segmentation)

and finally: calorimeters contribute to **particle identification**
(type of interaction \rightarrow form of energy deposition)



Energy depositions measured in the UA2 experiment
(1984) $Z \rightarrow ee$ and $W \rightarrow ev$ candidate events

Calorimeters are essential components for LHC detectors
(energy measurement of electrons, photons, jets, taus, missing transverse momentum,
muon identification)

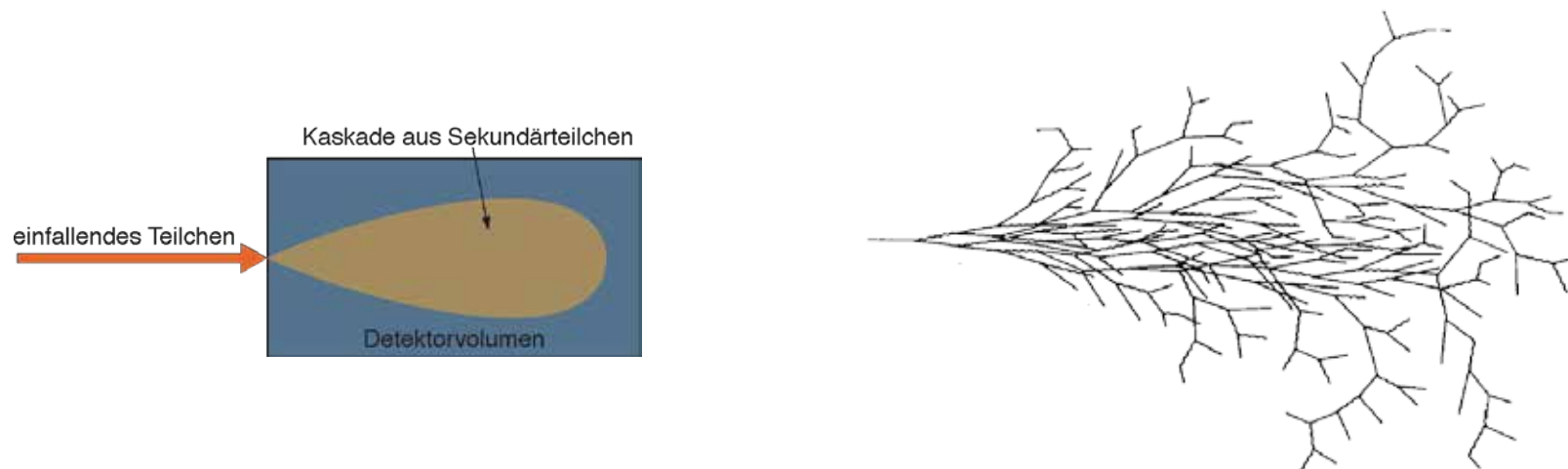


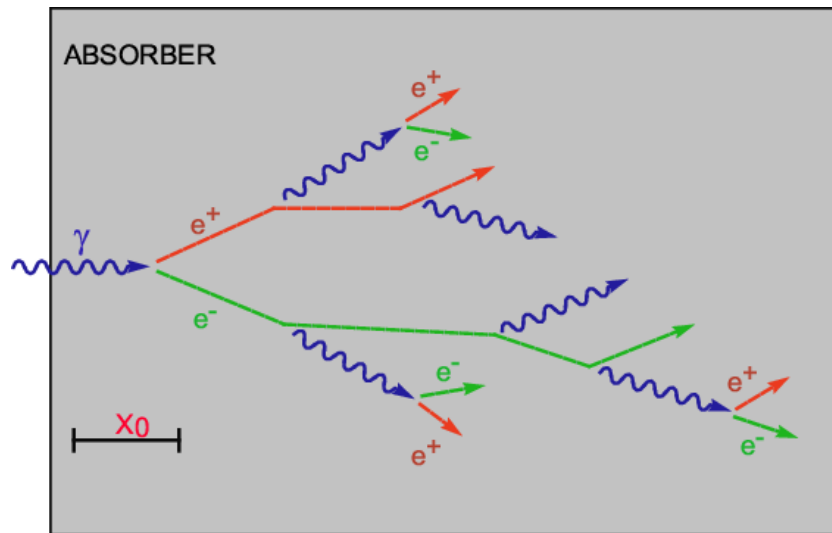
Principle of operation:

- Energy is transferred to an **electrical signal** (ionization charge) or to a **light signal** (scintillators, Cherenkov light)
- This **signal** should be **proportional to the original energy**: $E = \alpha S$
Calibration procedure $\rightarrow \alpha$ [GeV / S]
- Energy of primary particle is transferred to new particles
 \rightarrow cascade / shower of new, lower energy particles

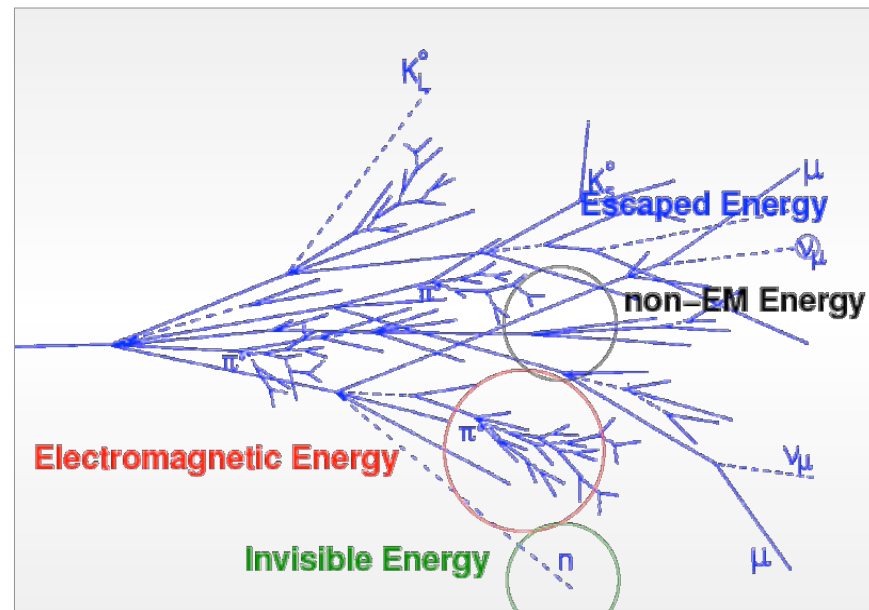
The shower development is determined by the type of the incoming particle and the corresponding interaction;

One distinguishes between electromagnetic showers (e, γ) and hadronic showers (initiated by all hadrons, inelastic hadronic interactions)





Schematic of an electromagnetic calorimeter shower initiated by a photon

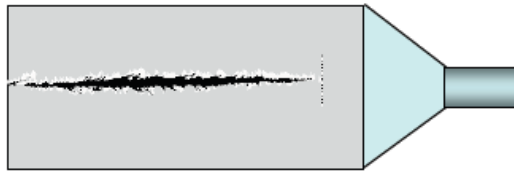


Schematic of a hadronic calorimeter shower

Two principal calorimeter layouts:

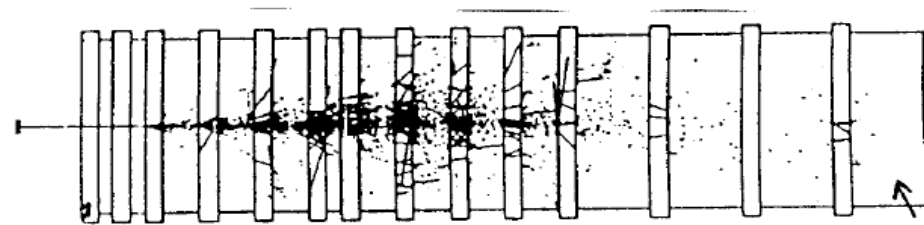
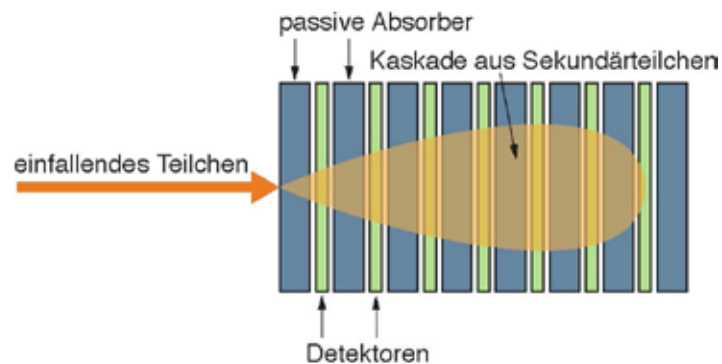
(1) Homogeneous calorimeter

One material serves to absorb the energy and to provide the measureable signal (e.g. lead glass block, scintillator block, liquid argon volume)



(2) Sampling calorimeter

Absorber material (passive) (Fe, Pb, Cu, ...)
+ Sensitive / detector medium (Liquid argon, scintillators, gas ionization detectors)



Important parameters of a calorimeter:

- **Linearity** of the energy measurement
- Precision of the energy measurement (**resolution**, $\Delta E / E$)
in general limited by fluctuations in the shower process

worse for sampling calorimeters as compared to homogeneous calorimeters

- Uniformity of the energy response to different particles (**e/h response**)

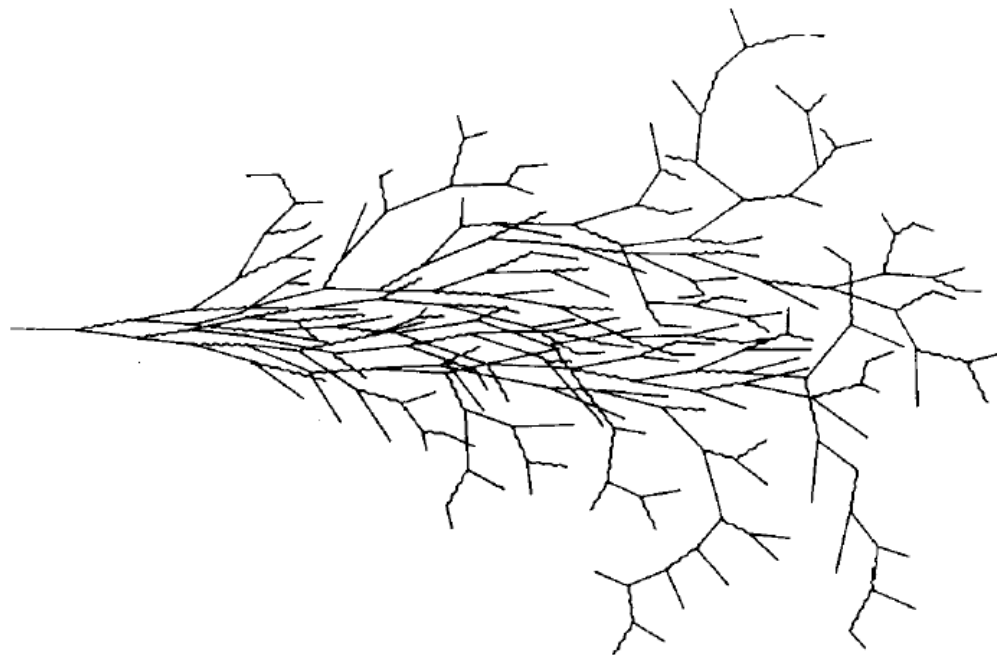
in general: response of calorimeters is different to electromagnetically interacting particles (e, γ) and hadrons (h)

Further calorimeter features:

- **Good energy resolution at high energy:** the relative energy resolution decreases as $1/\sqrt{E}$
(in contrast to momentum measurement in tracking detectors, which scales with p_T ;
in addition: no direction dependence of energy resolution, unlike $1/\sin \theta$ resolution term in the momentum resolution)
- **Hermeticity:** calorimeters can be built nearly as 4π -detectors
i.e. they can measure the energy of charged and neutral particles over almost the full solid angle
→ important for the measurement of the (missing) transverse energy
- **Trigger / timing capabilities:** calorimeters can provide fast timing signals (1 – 20 ns)
→ they can be used for triggering

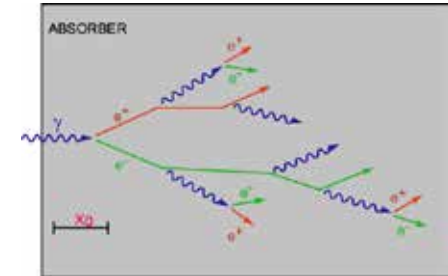
ATLAS + CMS: fast (Level-1) trigger signals from calorimeters and fast muon trigger stations

8.2 Electromagnetic calorimeter showers



Overview of interaction processes of electrons and photons

For high energies: bremsstrahlung and pair creation dominate
doubling of particles → shower development



Energy loss due to excitation and ionisation

Bethe Bloch formula

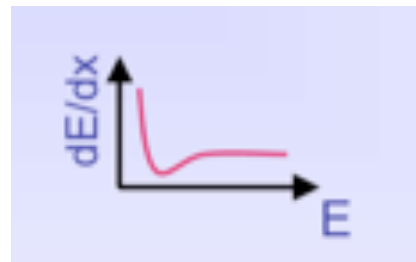
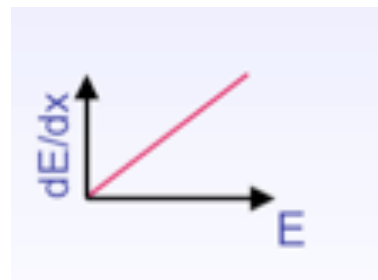


Photo effect

(dominant in ~ keV energy range)



Bremsstrahlung



Compton effect

(dominant in MeV energy range)



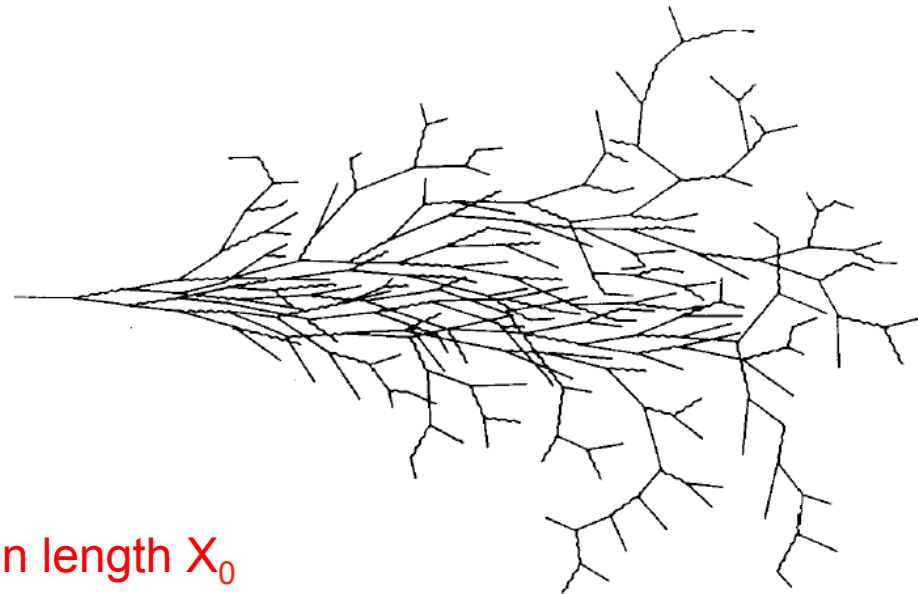
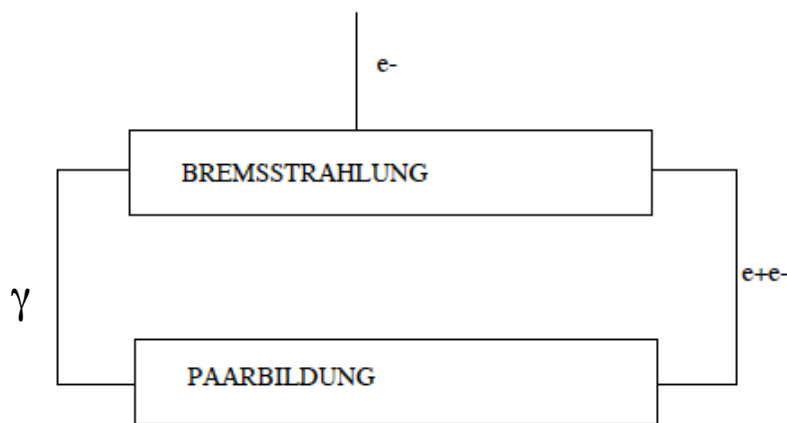
Cherenkov radiation

Pair creation

(threshold energy
= $2 m_e = 1,022 \text{ MeV}$)



- Particle showers created by electrons/positrons or photons are called electromagnetic showers (only electromagnetic interaction involved)
- Basic processes for particle creation: bremsstrahlung and pair creation



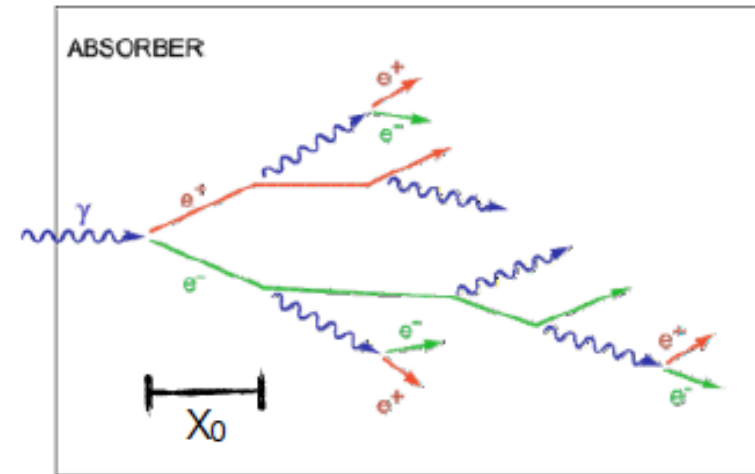
- Characteristic interaction length: **radiation length X_0**
- Number of particles in the shower increases, until the critical energy E_c is reached; For $E < E_c$ the energy loss due to ionization and excitation dominates, the number of particles decreases, due to stopping in material

Reminder: e/γ processes

Dominant processes
at high energies ...

Photons : Pair production

Electrons : Bremsstrahlung



Pair production:

$$\sigma_{\text{pair}} \approx \frac{7}{9} \left(4 \alpha r_e^2 Z^2 \ln \frac{183}{Z^{1/3}} \right)$$

$$= \frac{7}{9} \frac{A}{N_A X_0} \quad [X_0: \text{radiation length}]$$

[in cm or g/cm²]

Absorption
coefficient:

$$\mu = n\sigma = \rho \frac{N_A}{A} \cdot \sigma_{\text{pair}} = \frac{7}{9} \frac{\rho}{X_0}$$

Bremsstrahlung:

$$\frac{dE}{dx} = 4\alpha N_A \frac{Z^2}{A} r_e^2 \cdot E \ln \frac{183}{Z^{1/3}} = \frac{E}{X_0}$$

$$\rightarrow E = E_0 e^{-x/X_0}$$

After passage of one X_0 electron
has only $(1/e)^{\text{th}}$ of its primary energy ...

[i.e. 37%]

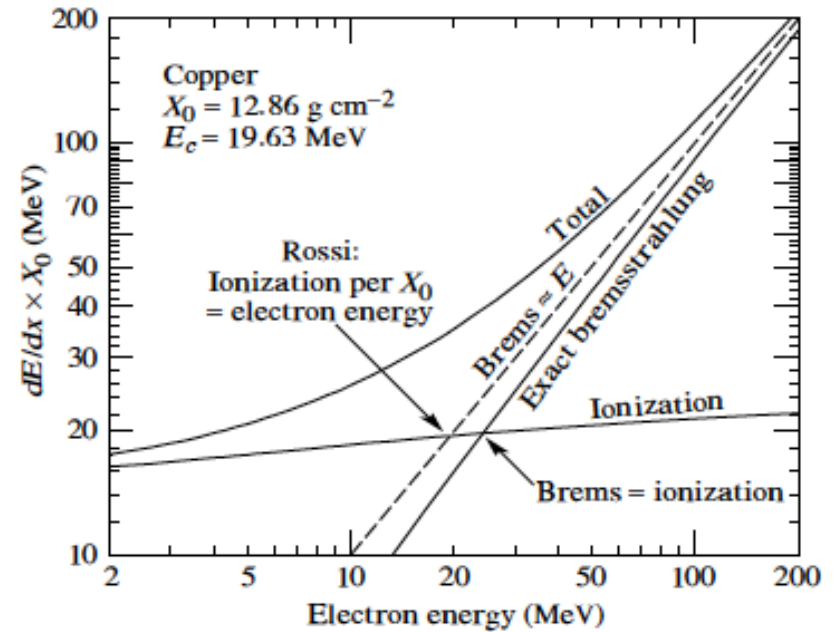
Critical Energy [see above]:

$$\left. \frac{dE}{dx}(E_c) \right|_{\text{Brems}} = \left. \frac{dE}{dx}(E_c) \right|_{\text{Ion}}$$

Approximations:

$$E_c^{\text{Gas}} = \frac{710 \text{ MeV}}{Z + 0.92} \quad \left[E_c^{\text{Sol/Liq}} = \frac{610 \text{ MeV}}{Z + 1.24} \right]$$

$$\left(\frac{dE}{dx} \right)_{\text{Brems}} / \left(\frac{dE}{dx} \right)_{\text{Ion}} \approx \frac{Z \cdot E}{800 \text{ MeV}}$$



with:

$$\left. \frac{dE}{dx} \right|_{\text{Brems}} = \frac{E}{X_0} \quad \& \quad \left. \frac{dE}{dx} \right|_{\text{Ion}} \approx \frac{E_c}{X_0} = \text{const.}$$

Transverse size of EM shower given by radiation length via Molière radius

[see also later]

$$R_M = \frac{21 \text{ MeV}}{E_c} X_0$$

R_M : Molière radius
 E_c : Critical Energy
 X_0 : Radiation length

The longitudinal shower shape

- The longitudinal shower formation can be calculated in detailed Monte Carlo simulation, taking into account the proper interaction processes and their energy dependence;

A simple model, to illustrate the relations given below, will be discussed later and in more detail in the tutorials

- The longitudinal energy deposition can be well described by the relation

$$\frac{dE}{dt} = E_0 t^\alpha e^{-\beta t}$$

α, β : free parameters

t^α : at small depth number of secondaries increases ...

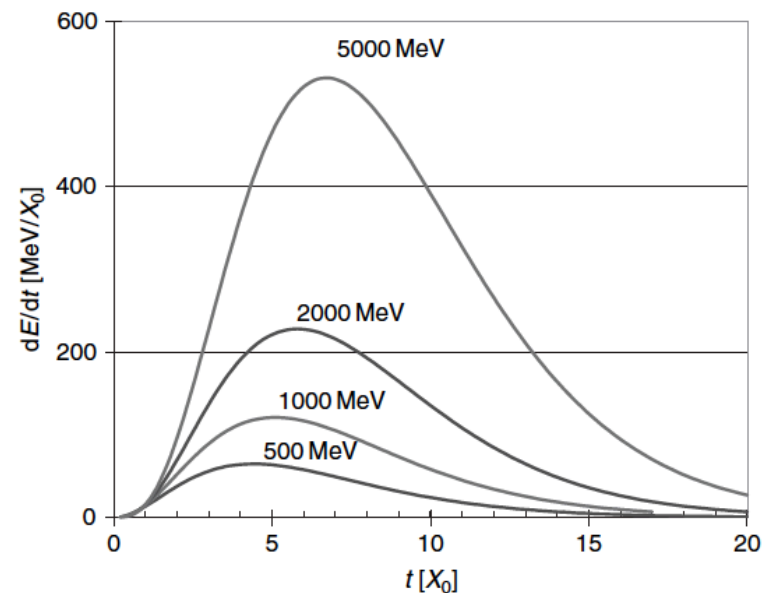
$e^{-\beta t}$: at larger depth absorption dominates ...

Numbers for $E = 2$ GeV (approximate):

$$\alpha = 2, \beta = 0.5, t_{\max} = \alpha/\beta$$

where $t =$ shower depth in units of X_0

t_{\max} = depths where the energy deposition is maximal



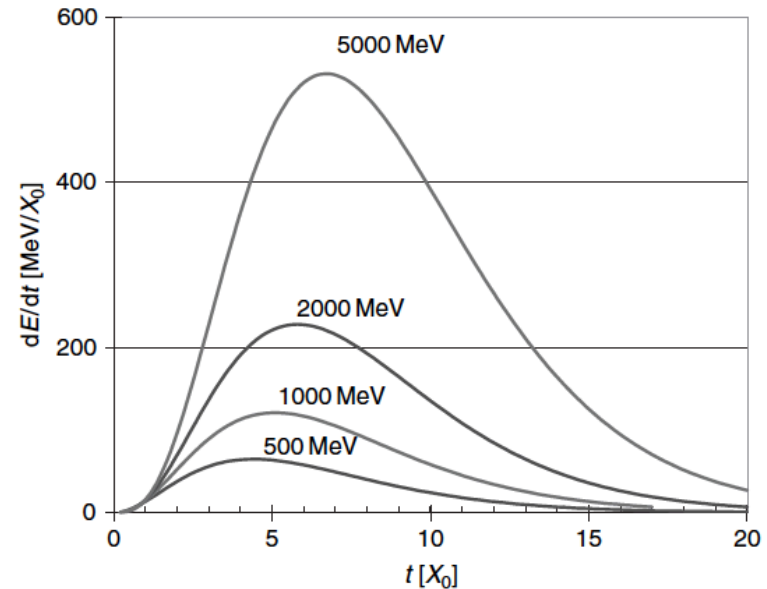
The longitudinal shower shape

More exact (EGS simulation and measurements)
 [Longo 1985]

$$\frac{dE}{dt} = E_0 \cdot \beta \cdot \frac{(\beta t)^{\alpha-1} e^{-\beta t}}{\Gamma(\alpha)}$$

[Γ: Gamma function]

where t = shower depth in units of X₀



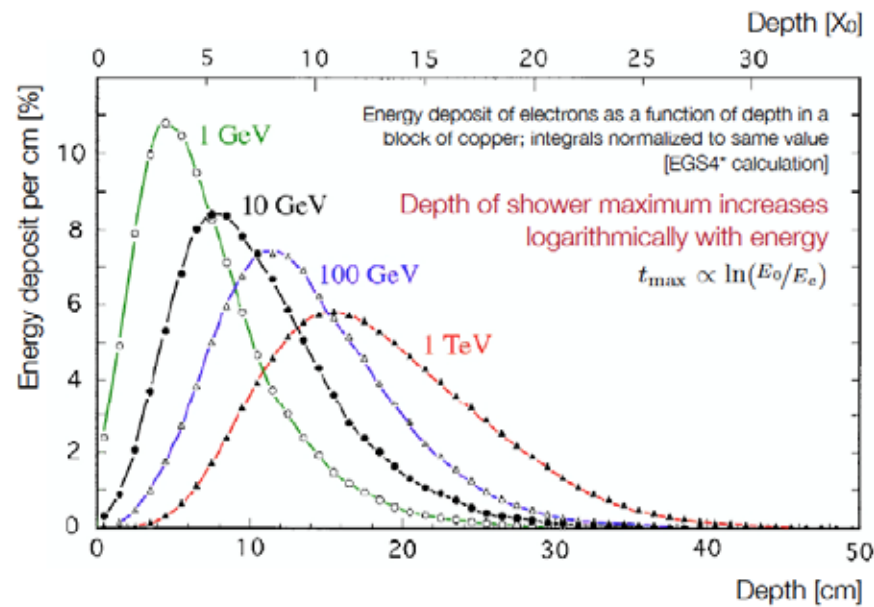
- For small t (beginning of the shower): the particle multiplicity and thereby the deposited energy grows
- At the end of the shower, the **number of particles** and thereby the energy deposition decreases since absorptive processes (Compton and photo effect for photons, stopping of electrons by dE/dx due to ionization) dominate *
- The **shower maximum** is found to grow logarithmically with the energy E₀ of the incident particle

$$t_{\max} = \frac{\alpha - 1}{\beta} = \ln \left(\frac{E_0}{E_c} \right) + C_{e\gamma} \quad \text{with } C_{e\gamma} = +0.5 \text{ for photon-induced showers} \\ = -0.5 \text{ for electron-induced showers}$$

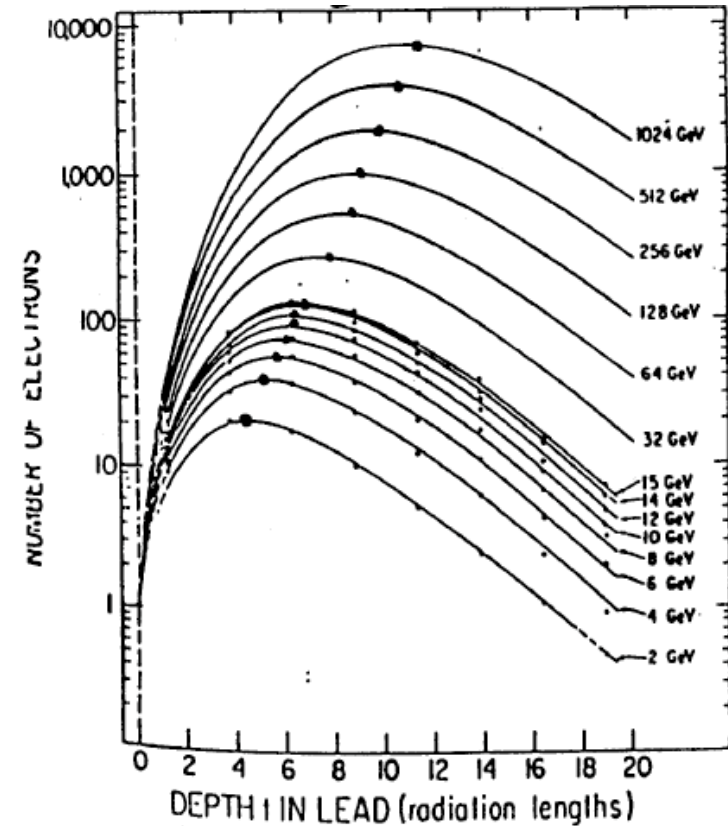
→ important practical implication: calorimeters grow only logarithmically with the energy of the particles to be absorbed

* It should be noted that for the energy deposition the total track length of all charged particles is relevant ! thereby the particle multiplicity (# charged particles) plays an essential role

The longitudinal shower shape



*EGS = Electron Gamma Shower



The longitudinal shower shape

Photons:

Photo-electric effect ...

$$\sigma \propto Z^5, E^{-3}$$

Compton scattering ...

$$\sigma \propto Z, E^{-1}$$

Pair production ...

σ increases with E, Z
asymptotic at ~ 1 GeV

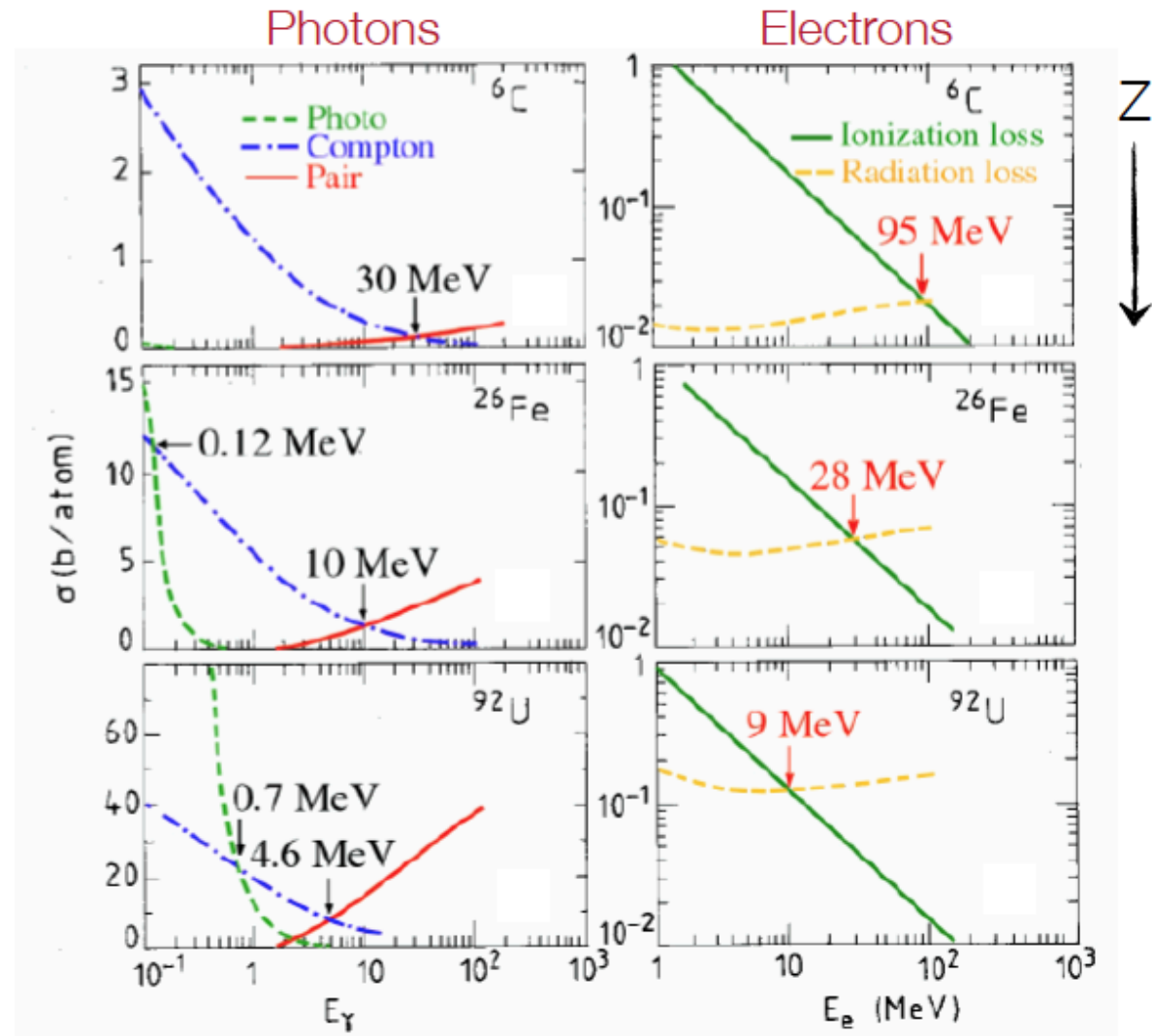
Electrons:

Critical energy ...

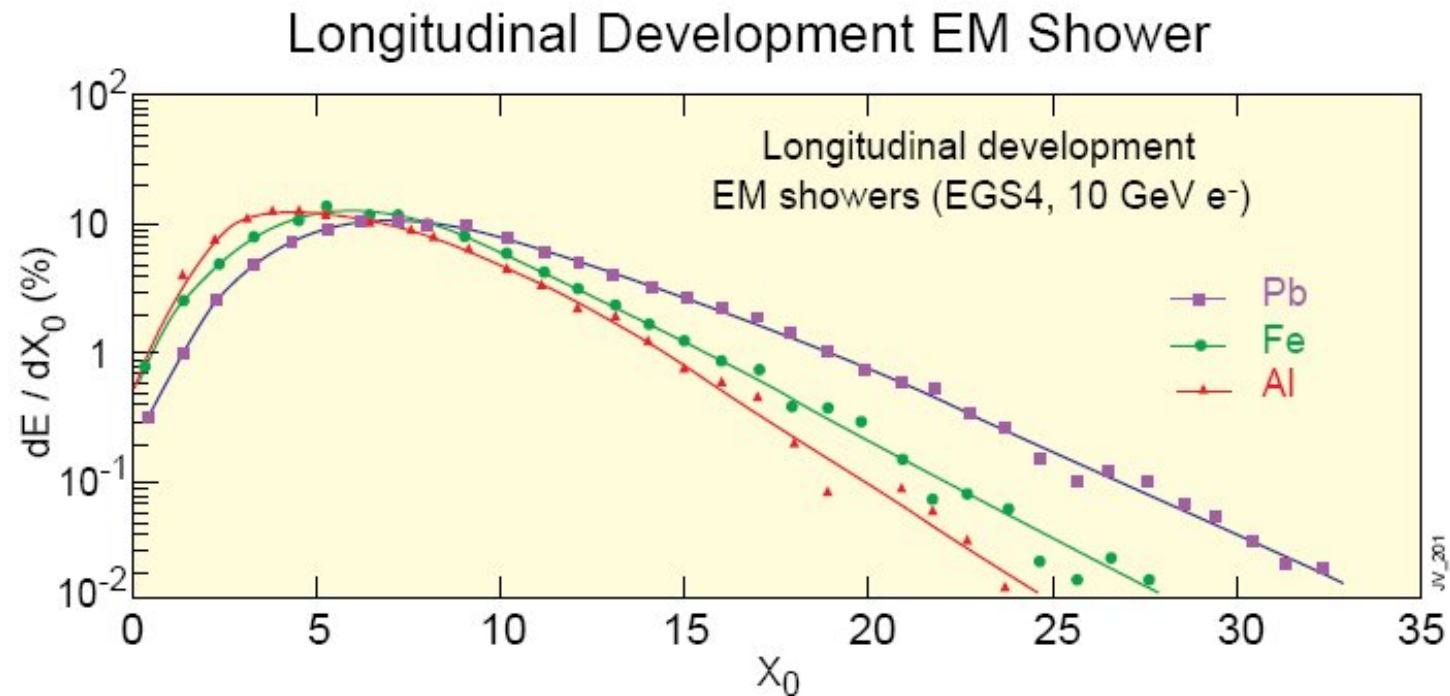
$$E_c \propto \frac{1}{Z}$$

In high Z materials
particle multiplication ...
... down to lower energies

→ longer showers
[with respect to X_0]



The longitudinal shower shape



Rough scaling law for longitudinal containment:

$$L(95\%) = t_{\max} + 9.6 + 0.08 Z \quad [X_0]$$

Lateral shower profile:

- The lateral shower profile is dominated by two processes:
 - Multiple Coulomb scattering
 - Relatively long free path length of low energy photons

(It should be noted that the opening angle of the two particles for bremsstrahlung and pair production is very small at high energies $\sim 1/\gamma^2$)

- The lateral width of the shower increases with the depth of the shower (→ figure)

(lower energy photons and electrons, multiple scattering effects are larger, long path length)

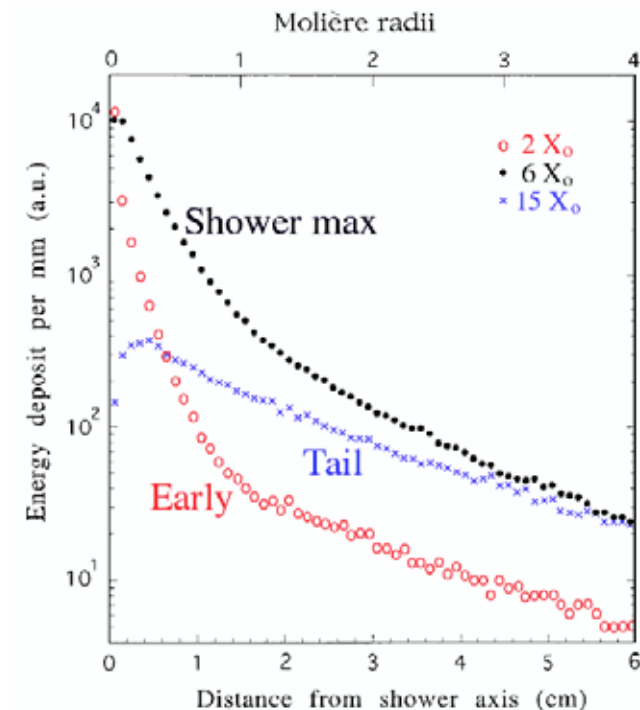
- The lateral shower profile is characterized by the so-called Molière radius ρ_M

$$\rho_M = \frac{21\text{MeV}}{E_C} X_0 \approx 7 \frac{A}{Z} \left[\frac{g}{\text{cm}^2} \right]$$

- About 95% (90%) of the shower energy are contained within a cylinder with radius $r = 2 \rho_M$ ($r = 1 \rho_M$)

→ well collimated !

Radial distribution of the energy deposited by 10 GeV electrons in copper (EGS simulation)



Broadening due to:

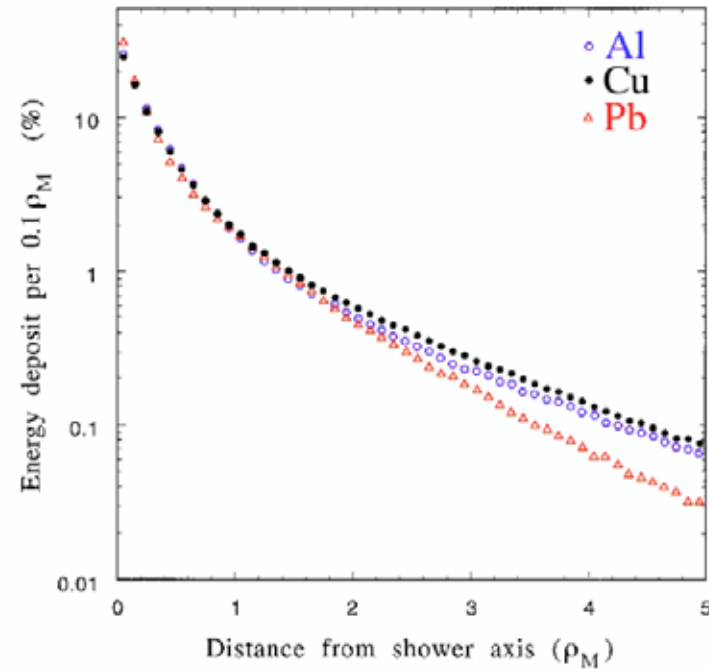
- multiple scattering (~up to shower maximum)
- low energy photons (~beyond shower maximum)

Lateral shower profile:

Material dependence of shower shape:

- Core shower shape are largely material independent
 - 95% containment within $2 \rho_M$ holds independently of material
- Tails are smaller for high-Z materials due to smaller mean free path length of low-energy photons (photo effect $\sim Z^5$)

Radial distribution of the energy deposited by 10 GeV electrons in Al, Cu, and Pb (EGS simulation)



Lateral shower profile:

- Example: Electromagnetic showers in lead glass (OPAL detector at LEP)

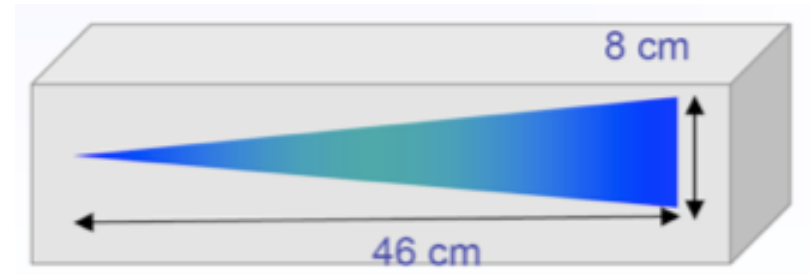
$$X_0 \approx 2 \text{ cm}, E_C = 11.8 \text{ MeV}, \rho_M = 1.8 X_0 \approx 3.6 \text{ cm}$$

For $E_0 = 100 \text{ GeV}$ one obtains:

$$t_{\text{max}} \approx 13$$

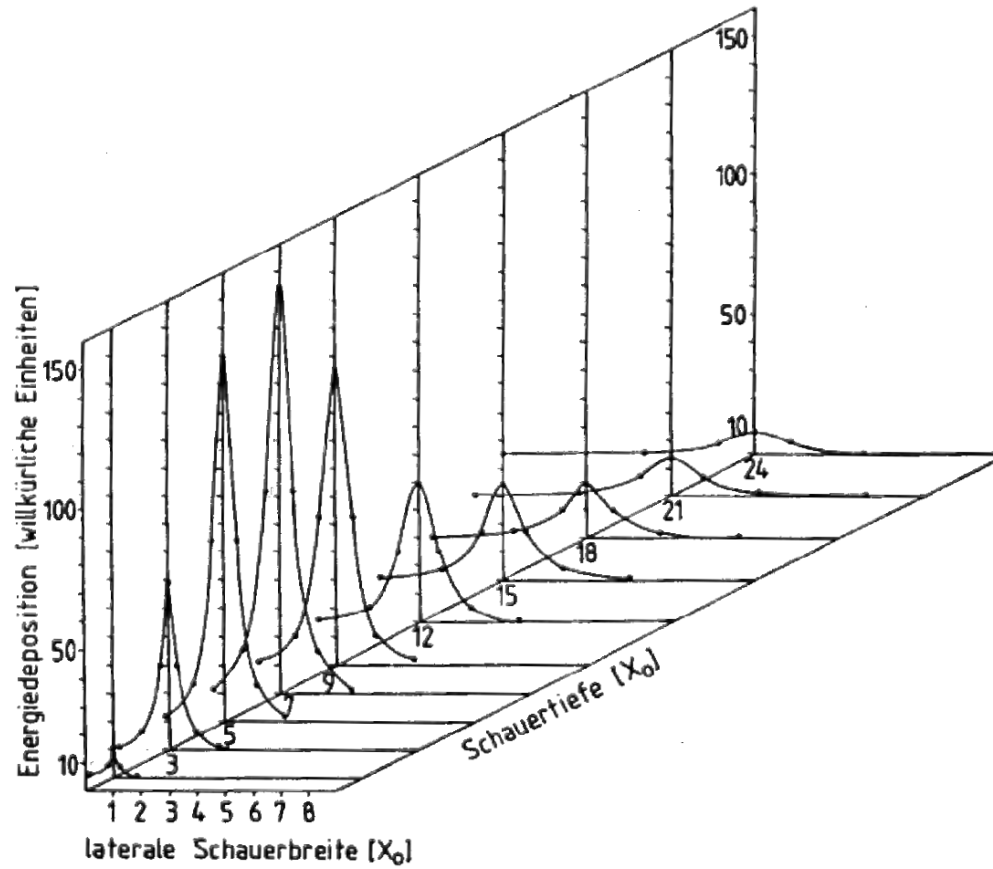
Longitudinal containment: $t_{95\%} \approx 23 = 46 \text{ cm}$

Lateral containment: $R_{95\%} = 2 \rho_M = 7.2 \text{ cm}$

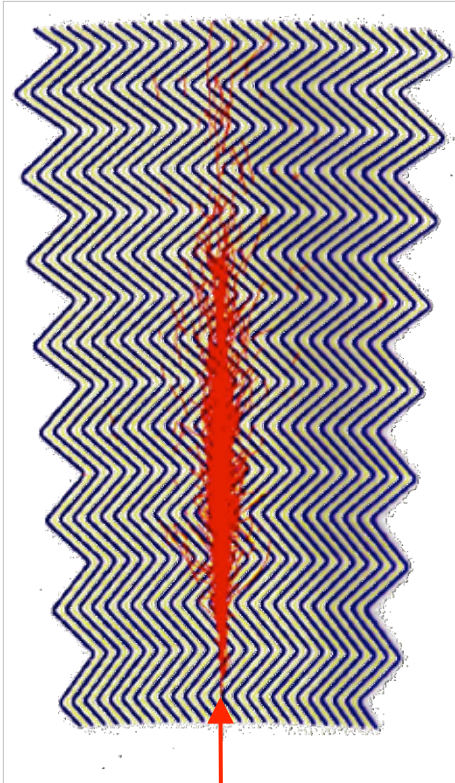


- The compact electromagnetic showers explain the dimensions (thickness and lateral granularity) of the electromagnetic calorimeters
 - perfect e/γ ID criteria: compact collimated showers
 - small lateral shower radii
 - very small leakage into the hadronic compartment of the calorimeter

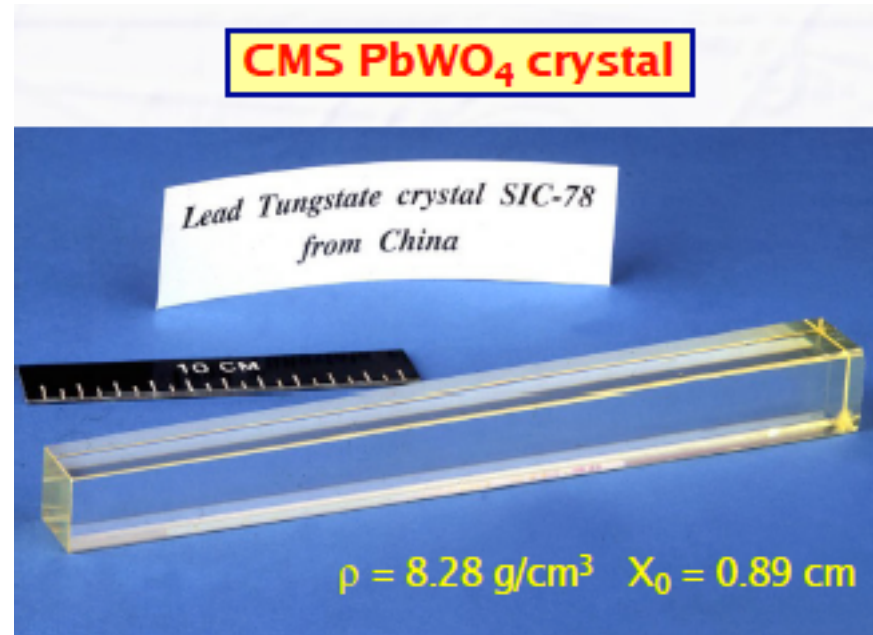
*Longitudinal and lateral shower profile
for electromagnetic showers*



The longitudinal and lateral shower profile for a 6 GeV electron in a lead absorber (from Ref. [3])



A GEANT / EGS simulation of a 40 GeV electron shower in the ATLAS Liquid Argon accordion calorimeter)



A PbWO_4 crystal of the CMS electromagnetic calorimeter

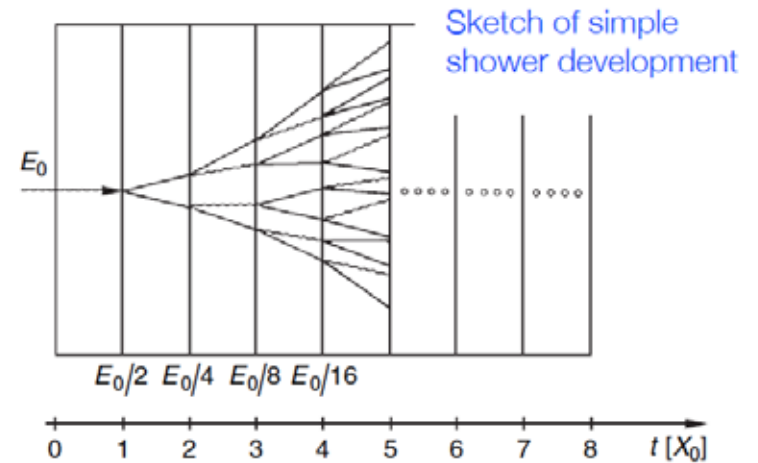
A simple shower model

- To illustrate the main features of electromagnetic showers:
 - Number of particles in the shower
 - Location of the shower maximum
 - Longitudinal and transverse shower shape
- Consider only bremsstrahlung and pair production
 - $E > E_c$: no energy loss by ionization / excitation
 - $E < E_c$: energy loss only via ionization

Simplification of symmetric energy sharing:

Bremsstrahlung: $E_\gamma = E_e = E_0/2$

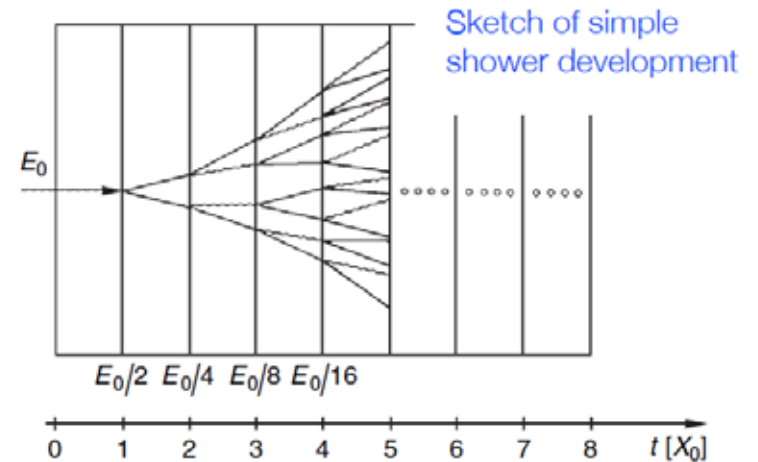
Pair creation: $E_e = E_0/2$



t = track length in units of X_0

A simple shower model

→ exercises



Number of shower particles
after depth t :

$$N(t) = 2^t$$

Energy per particle
after depth t :

$$E = \frac{E_0}{N(t)} = E_0 \cdot 2^{-t}$$

$$\rightarrow t = \log_2(E_0/E)$$

Total number of shower particles
with energy E_1 :

$$N(E_0, E_1) = 2^{t_1} = 2^{\log_2(E_0/E_1)} = \frac{E_0}{E_1}$$

Number of shower particles
at shower maximum:

$$N(E_0, E_c) = N_{\max} = 2^{t_{\max}} = \frac{E_0}{E_c}$$

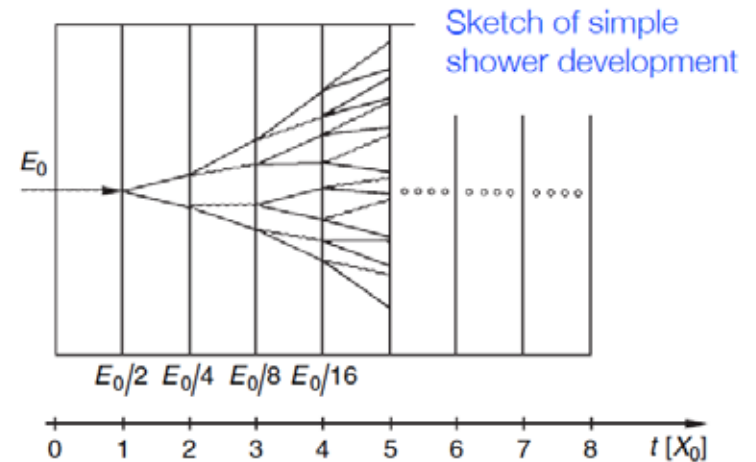
Shower maximum at:

$$t_{\max} \propto \ln(E_0/E_c)$$

$$\propto E_0$$

A simple shower model

→ exercises



Relevant for energy measurement (e.g. via scintillation light):
total integrated track length of all charged particles ...

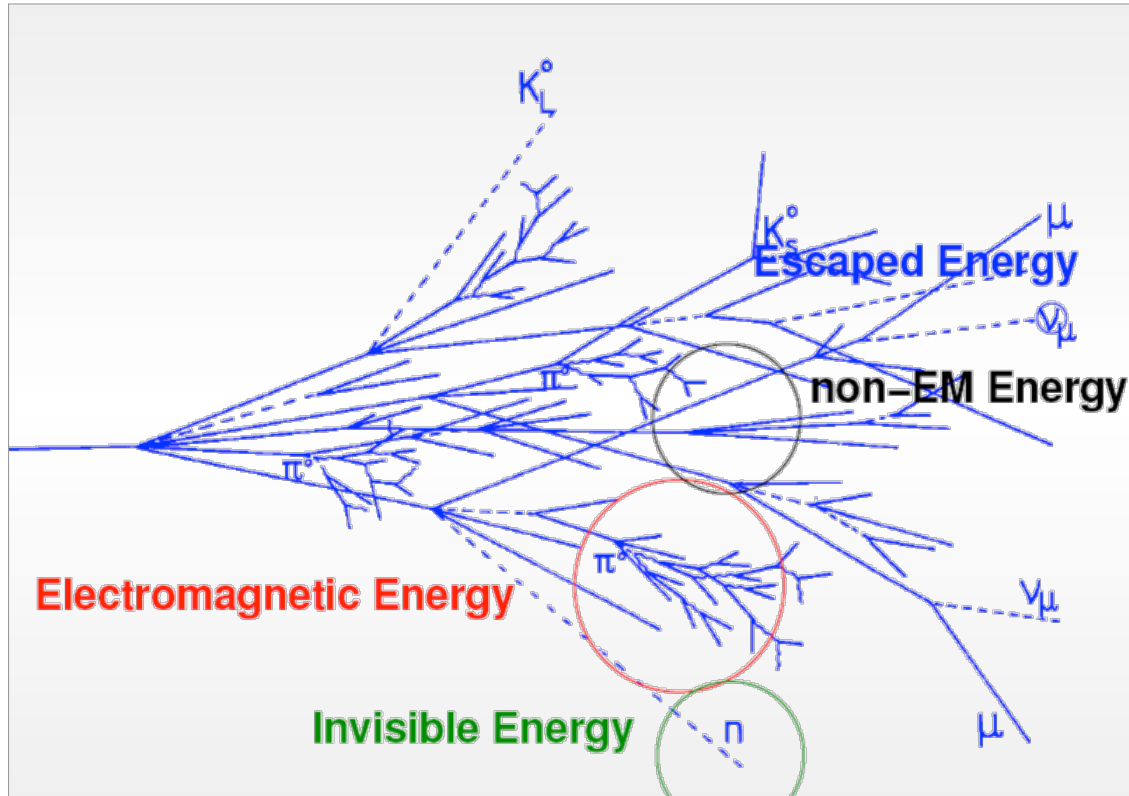
$$\begin{aligned}
 T &= X_0 \sum_{\mu=0}^{t_{\max}-1} 2^\mu + t_0 \cdot N_{\max} \cdot X_0 && \text{with } t_0: \text{ range of electron with energy } E_0 \\
 &= X_0 \cdot (2^{t_{\max}} - 1) + t_0 \cdot \frac{E_0}{E_c} X_0 && \text{[given in units of } X_0] \\
 &= X_0 \cdot (2^{\log_2 E_0/E_c} - 1) + t_0 \cdot \frac{E_0}{E_c} X_0 \approx (1 + t_0) \cdot \frac{E_0}{E_c} X_0 \propto E_0
 \end{aligned}$$

As only electrons
contribute ...

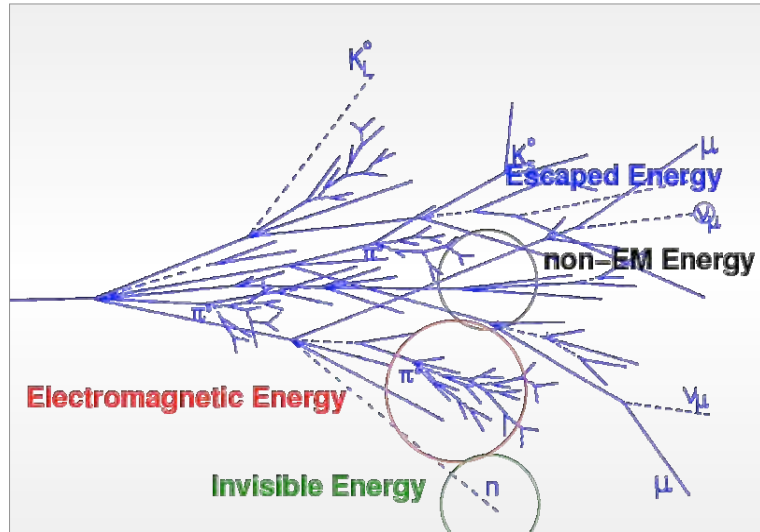
$$T = \frac{E_0}{E_c} \cdot X_0 \cdot F \quad [\text{with } F < 1]$$

Energy proportional
to track length ...

8.3 Hadronic calorimeter showers



- Hadrons initiate their energy showers by inelastic hadronic interactions; (strong interaction, showers are called **hadronic showers**)
- Hadronic showers are much more complex than electromagnetic showers

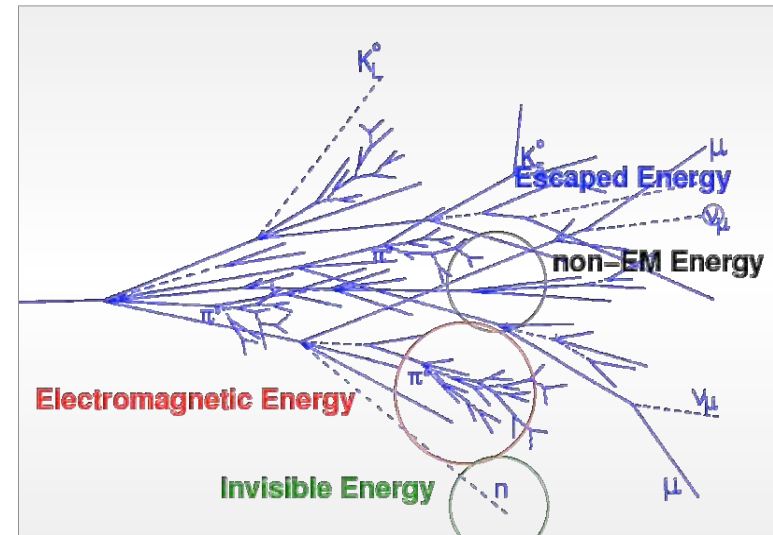


- Several secondary particles, meson production, multiplicity increases with energy $\sim \ln(E)$

The secondary hadrons undergo further inelastic collisions until their energy falls below the pion production threshold

- π^0 components, $\pi^0 \rightarrow \gamma\gamma$, **electromagnetic sub-showers**;
The fraction of the electromagnetic component grows with energy,
 $f_{EM} = 0.1 \ln E$ (E in GeV, in the range $10 \text{ GeV} < E < 100 \text{ GeV}$)

- Exited nuclei
 - β decays, γ decays
- Neutron capture → nuclear fission
 - excited fission products
 - further β and γ decays
- Decays of particles
(slow particles at the end of the shower)
 - e.g. $\pi \rightarrow \mu \nu_\mu$
 - escaping particles → missing energy



Energy loss processes in hadron showers:

- During the hadronic interactions atomic nuclei are broken up or remain in excited states

The corresponding energy (excitation energy, binding energy) comes from the original particle energy

→ no or only partial contribution to the visible energy

(de-excitation has time constant, might be larger than electronic signal shaping time)

- Important **neutron component**

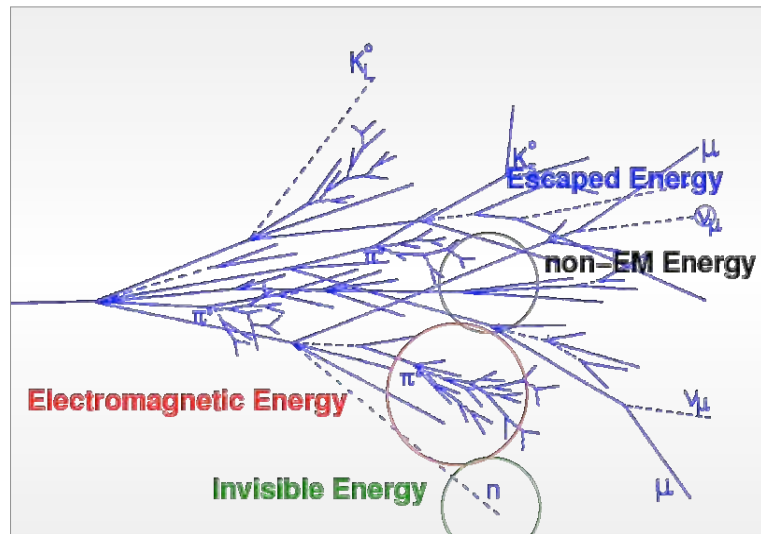
The interaction of neutrons depends strongly on their energy;

Extreme cases:

- Nuclear reaction, e.g. nuclear fission → energy recovered
 - Escaping the calorimeter (undergo only elastic scattering, without inelastic interaction)
- Decays of particles (as described above, e.g. $\pi \rightarrow \mu \nu_\mu$)
→ escaping particles → missing energy

These energy loss processes have important consequences:

In general, the response of the calorimeter to electrons/photons and hadrons is different ! The signal for hadrons is non-linear and smaller than the e/γ signal for the same particle energy



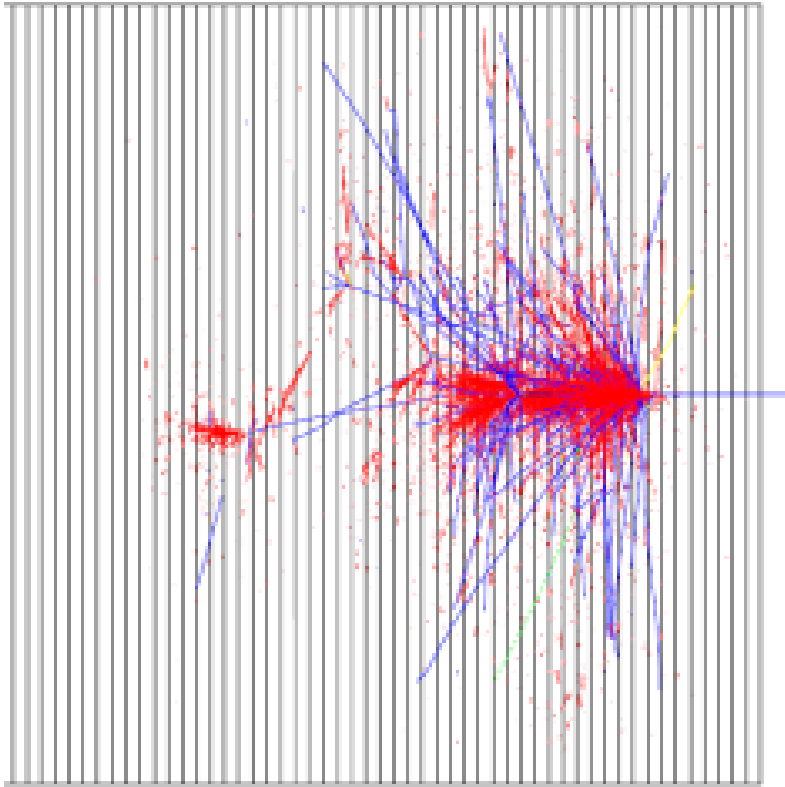
Typical energy balance (single event, GEANT simulation, large fluctuations from event-to-event):

[5 GeV proton in a lead-scintillator calorimeter]

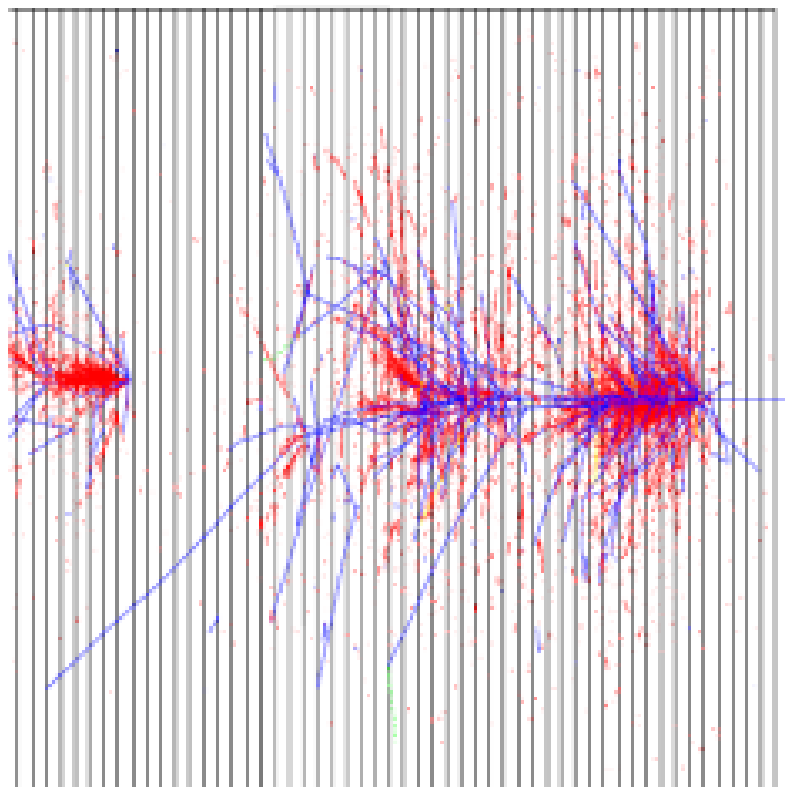
Ionization energy of charged particles (p, π, μ)	1980 MeV [40%]
Electromagnetic shower (π^0, η^0, e)	760 MeV [15%]
Neutrons	520 MeV [10%]
Photons from nuclear de-excitation	310 MeV [6%]
Non-detectable energy (nuclear binding, neutrinos)	1430 MeV [29%]
	5000 MeV

Two hadronic showers in a sampling calorimeter

1.



2.



Red: electromagnetic component
Blue: charged hadron component

Hadronic showers show very large fluctuations from one event to another
→ expected worse energy resolution

The basic cross section for hadronic interactions is the **total inelastic pp cross section**:

$$\sigma_{\text{tot}} = \sigma_{\text{el}} + \sigma_{\text{inel}} \quad *)$$

(For 1 – 100 GeV range inelastic processes dominate)

$$\sigma_{\text{el}} \approx 10 \text{ mb}$$

$$\sigma_{\text{inel}} \sim A^{2/3} \text{ (geometrical cross section)}$$

For the total cross section on a **target with A nuclei**:

$$\sigma_{\text{tot}} (\text{pA}) \approx \sigma_{\text{tot}} (\text{pp}) A^{2/3}$$

The hadronic interaction length is given by (see Chapter 2):

$$\lambda_{\text{int}} = \frac{1}{\sigma_{\text{tot}} \cdot n} = \frac{A}{\sigma_{pp} A^{2/3} \cdot N_A \rho} \sim A^{1/3}$$

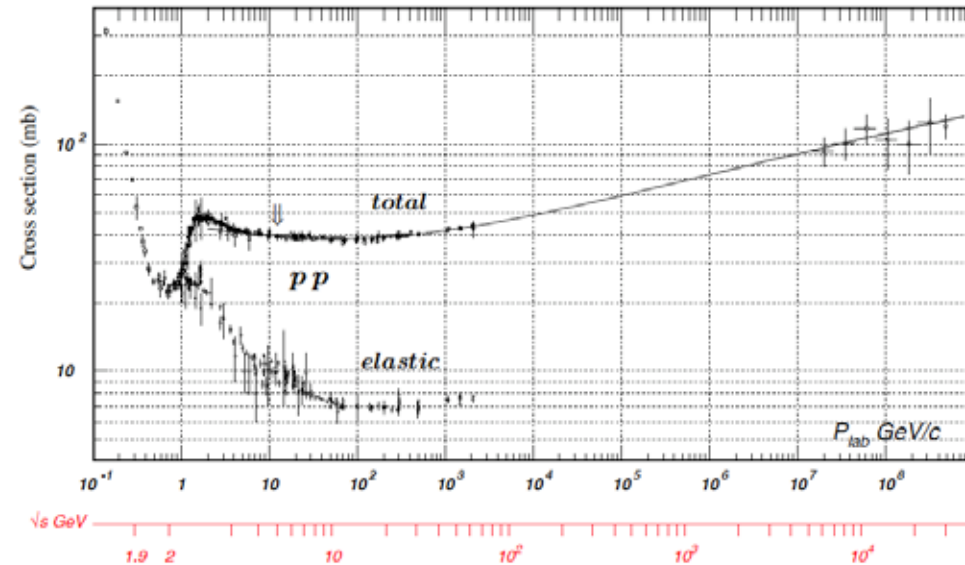
$$\approx 35 \text{ g/cm}^2 \cdot A^{1/3}$$

which yields:

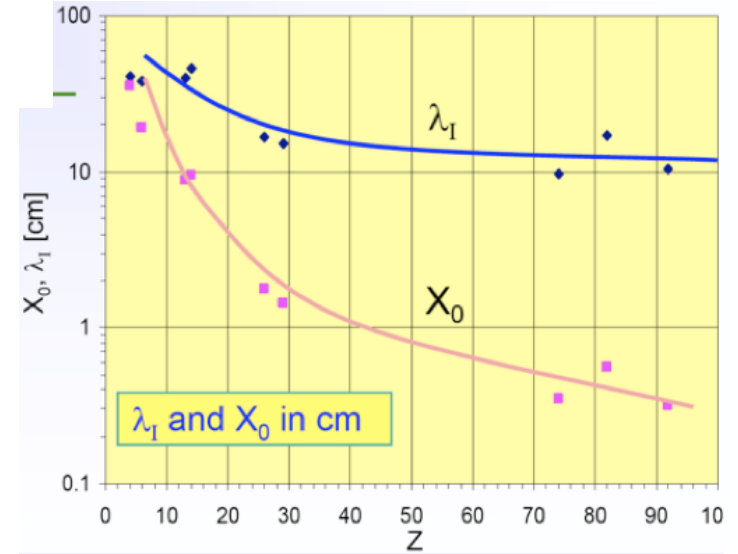
$$N(x) = N_0 \exp(-x/\lambda_{\text{int}})$$

*) diffractive processes neglected

Total proton-proton cross section
(pn cross section is similar in 1-100 GeV range)



Hadronic versus electromagnetic interaction lengths:



note: for high-Z materials (needed for an efficient absorption) the hadronic interaction lengths are about a factor 10-30 larger than the radiation lengths

→ much more material is needed to stop hadrons compared to electrons;

this explains the large extension of the hadronic calorimeters in large detector systems

Material	X_0 (cm)	λ_{had} (cm)
Liquid Argon Scintillator	14.0 42.2	83.7 79.4
Be	35.3	40.7
C	18.8	38.1
Fe	1.76	16.76
Cu	1.43	15.06
W	0.35	9.59
Pb	0.56	17.09
U	0.32	10.5

Hadronic shower development:
(estimates similar to e.m. case)

Depth (in units of λ_{int}):

$$t = \frac{x}{\lambda_{\text{int}}}$$

Energy in depth t:

$$E(t) = \frac{E}{\langle n \rangle^t} \quad \& \quad E(t_{\text{max}}) = E_{\text{thr}}$$

[with $E_{\text{thr}} \approx 290 \text{ MeV}$]

$$E_{\text{thr}} = \frac{E}{\langle n \rangle^{t_{\text{max}}}}$$

Shower maximum:

$$\langle n \rangle^{t_{\text{max}}} = \frac{E}{E_{\text{thr}}}$$

Number of particles
lower by factor E_{thr}/E_c
compared to e.m. shower ...

Intrinsic resolution:
worse by factor $\sqrt{E_{\text{thr}}/E_c}$

$$t_{\text{max}} = \frac{\ln(E/E_{\text{thr}})}{\ln \langle n \rangle}$$

This constitutes only a rough estimate since:

- The energy sharing between particles fluctuates strongly
- Part of the energy is not detectable
- Partial compensation (n-capture, fission)
- The electromagnetic energy fraction
(i.e. fraction of energy deposited by π^0 via $\pi^0 \rightarrow \gamma\gamma$ decays increases with energy

$$f_{em} \approx f_{\pi^0} \sim \ln E$$

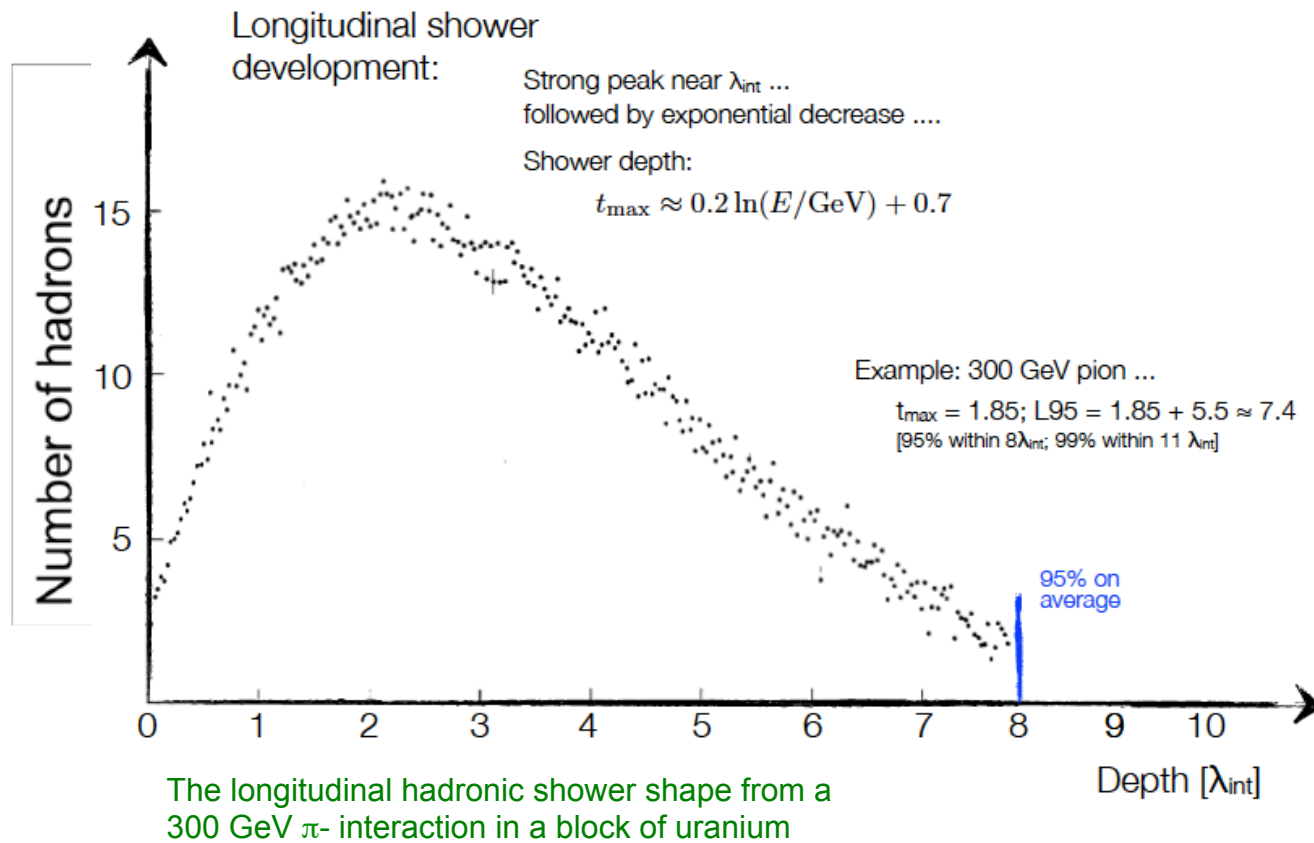
Explanation: neutral pions can be produced from π^-p reactions, via $\pi^-p \rightarrow \pi^0n$;
However, π^0 s do not contribute to the production of charged pions via $\pi^0p \rightarrow \pi^+n$ or $\pi^0n \rightarrow \pi^-p$ since they decay nearly promptly ($\tau \sim 10^{-16} \text{ s}$) into $\gamma\gamma$ before they can undergo hadronic interactions

The number of π^- increases logarithmically with the energy (multiplicity dependence)

- In the low energy tails also hadrons lose their energy mainly via ionization and excitation (dE/dx)

→ Detailed Monte Carlo simulations (GEANT with its various hadronic shower models) are needed to obtain a reasonable description of hadronic showers

The longitudinal hadronic shower shape

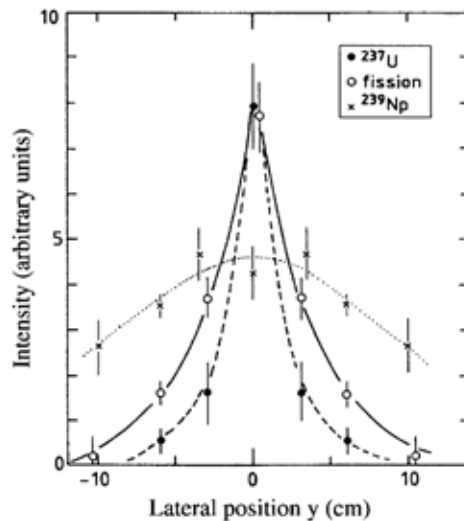
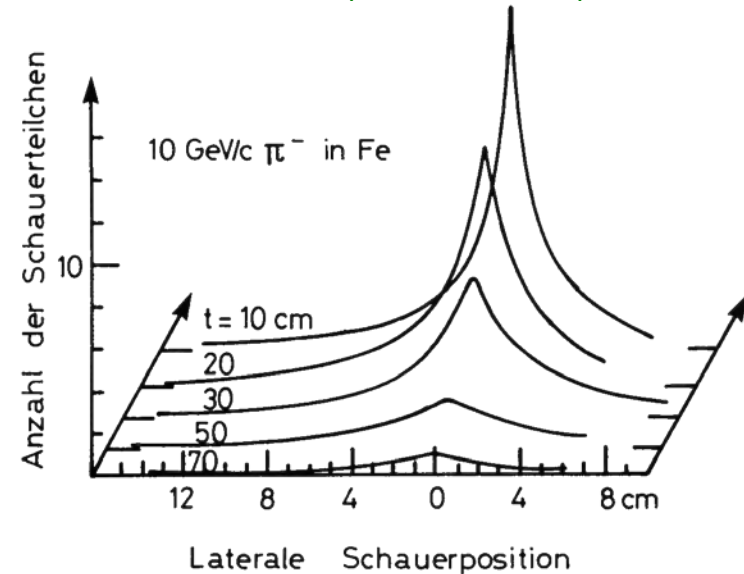


Typically $8\lambda_{\text{int}}$ are needed for a 95% hadronic shower containment of 300 GeV charged pions in uranium

The lateral hadronic shower shape

- Transverse shower sizes are larger for hadronic showers than for em showers
- They are determined by:
 - Transverse momenta of secondary particles $\langle p_T \rangle \approx 350 \text{ MeV}$
 - Free path length of secondary hadrons (λ_{int})
- Electromagnetic components lead to a relatively well-defined core
- Neutrons and charged pions form a wider core
- Thermal neutrons generate a broad tail

The lateral shower profile of 10 GeV pions in iron



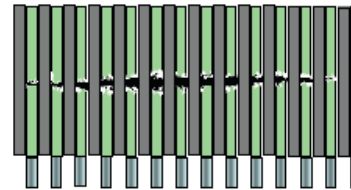
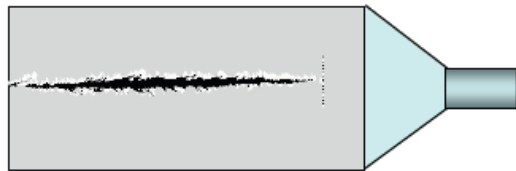
The various components can be separated by measuring the induced radioactivity:

- Fission (indicated by ^{99}Mo radioactivity, neutron induced); probes n component
- ^{237}U : mainly produced via $^{238}\text{U}(\gamma, n)^{237}\text{U}$; probes electromagnetic component
- ^{239}Np : produced by n-attachment from ^{238}U ; probes thermal neutron component

8.4 Layout and readout of calorimeters

- In general, one distinguishes between **homogenous calorimeters** and **sampling calorimeters**

For homogeneous calorimeters: absorber material = active (sensitive) medium



- Examples for **homogeneous calorimeters**:
 - NaJ or other crystals (BGO, BaF₂, CsF₃, ..) (Scintillation light)
 - Lead glass (Cherenkov light)
 - Liquid noble gases (Ar, Kr, Xe) (Ionization charge)
- Sampling calorimeters**: absorption and hadronic interactions occur mainly in dedicated absorber materials (dense materials with high Z, passive material) Signal is created in active medium, only a fraction of the energy contributes to the measured energy signal

Homogenous calorimeters

- + Provide a good energy resolution
- Very expensive
 - They are exclusively used for electromagnetic calorimeters (e, γ measurements)

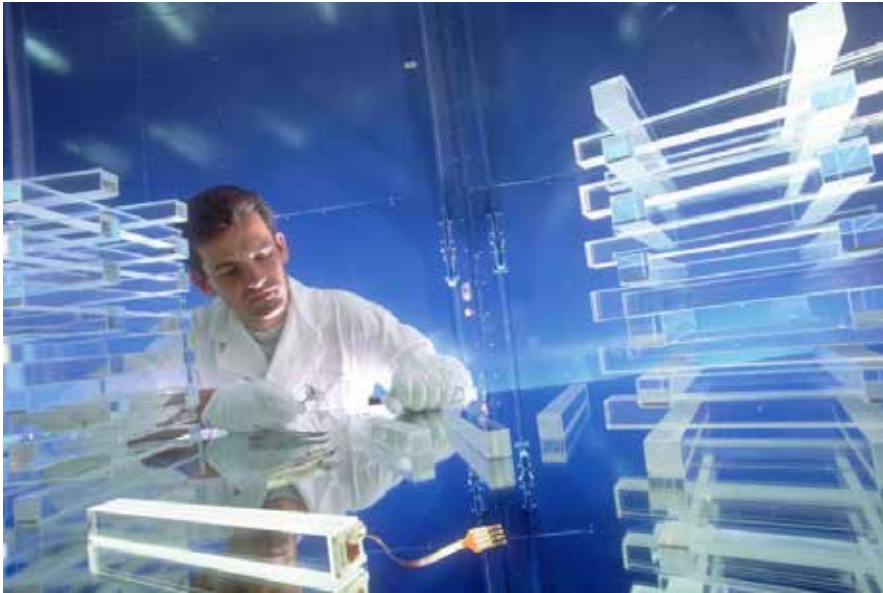
Sampling calorimeters

- + By freely choosing the high density absorber one can built more compact calorimeters
 - Cheaper than homogeneous calorimeters
- Only a fraction (typically a few %) of the deposited energy is actually detected in the active layers
 - A degraded energy resolution due to the fluctuations in the sampling

Properties of commonly used scintillator crystals in calorimetry:

Scintillator	Density [g/cm ³]	X ₀ [cm]	Light Yield γ/MeV (rel. yield*)	τ ₁ [ns]	λ ₁ [nm]	Rad. Dam. [Gy]	Comments
NaI (Tl)	3.67	2.59	4×10 ⁴	230	415	≥10	hygroscopic, fragile
CsI (Tl)	4.51	1.86	5×10 ⁴ (0.49)	1005	565	≥10	Slightly hygroscopic
CSI pure	4.51	1.86	4×10 ⁴ (0.04)	10 36	310 310	10 ³	Slightly hygroscopic
BaF ₂	4.87	2.03	10 ⁴ (0.13)	0.6 620	220 310	10 ⁵	
BGO	7.13	1.13	8×10 ³	300	480	10	
PbWO ₄	8.28	0.89	≈100	440 broad band 530 broad band		10 ⁴	light yield =f(T)

Example for a homogeneous calorimeter: CMS crystal calorimeter

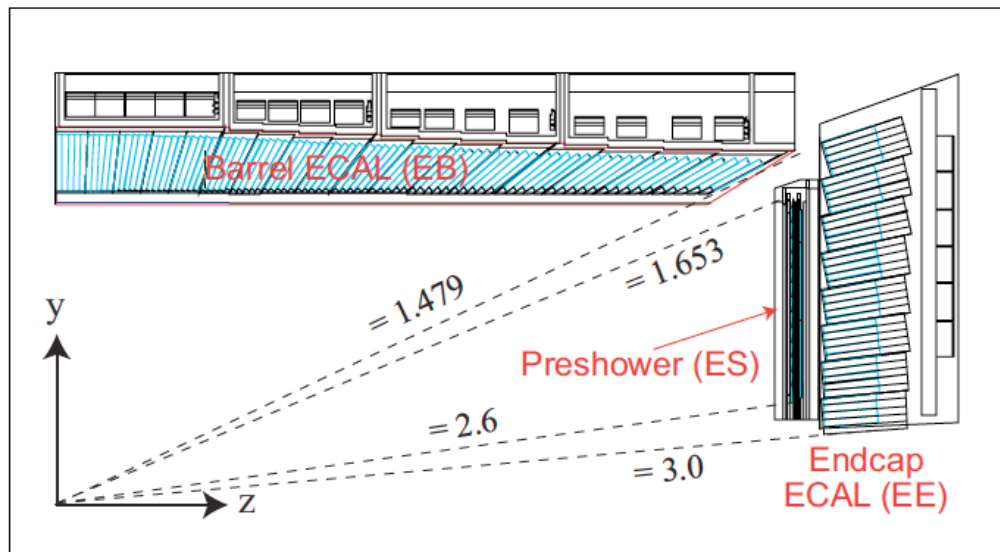


Scintillator: PbWO_4

Photo sensor: Avalanche photodiodes (APDs)

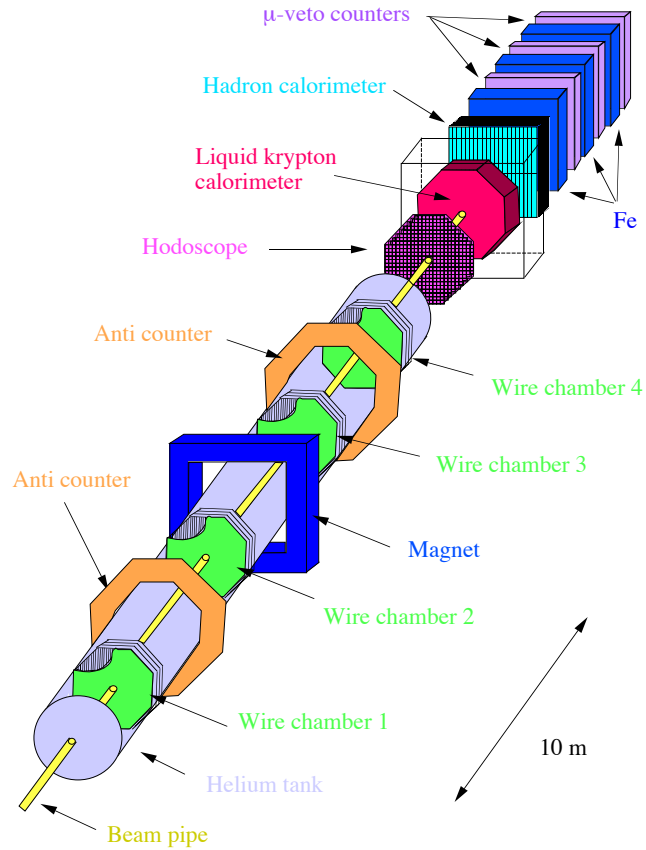
Number of crystals: ~ 70.000

Light output: 4.5 photons / MeV



Example 2: NA48 Liquid krypton calorimeter

The NA48 Detector

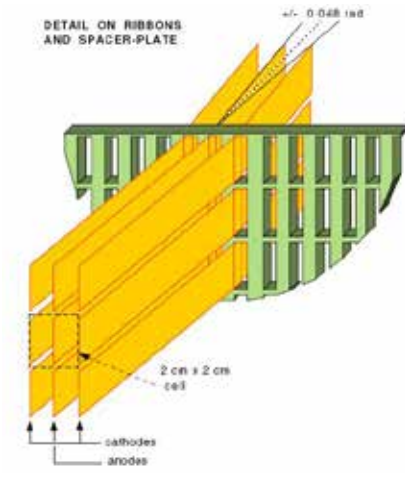
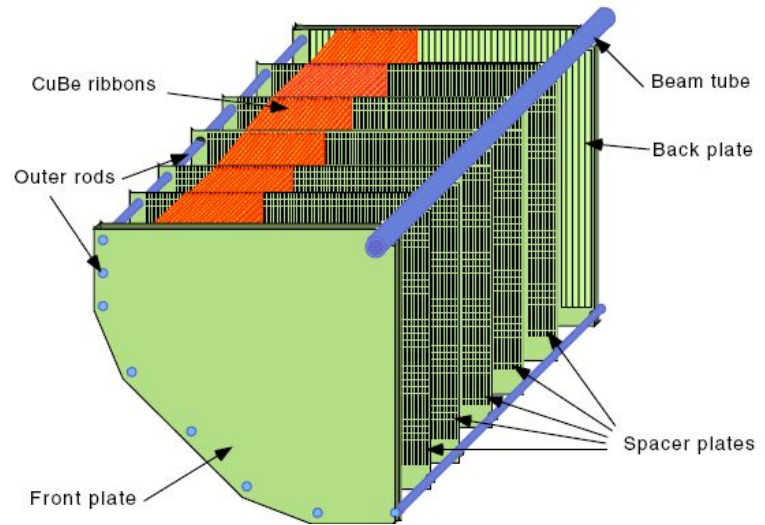


Full liquid krypton ($\sim 10 \text{ m}^3$)

Dimensions: 2.6 m diameter, 1.25 m depth = $27 X_0$

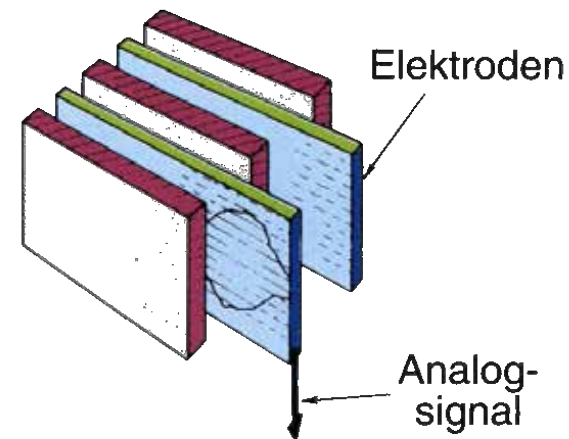
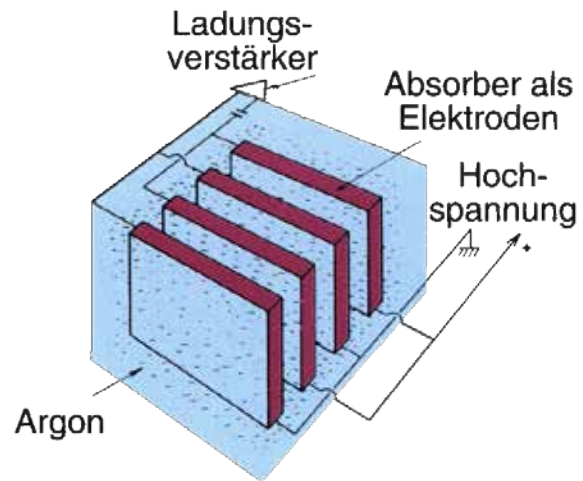
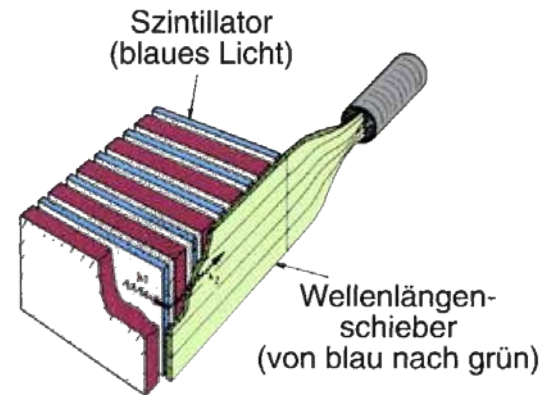
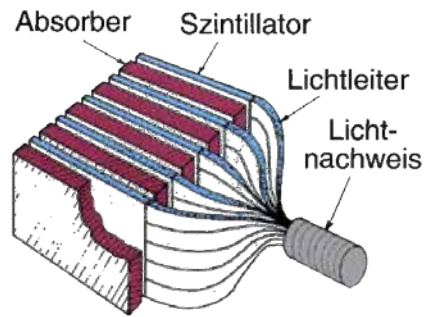
($X_0 = 4.7 \text{ cm}$, Molière radius $\rho_M = 4.7 \text{ cm}$)

The readout structure, electrodes, define the cells and the granularity here: $(2 \times 2 \text{ cm}^2)$ tower structure



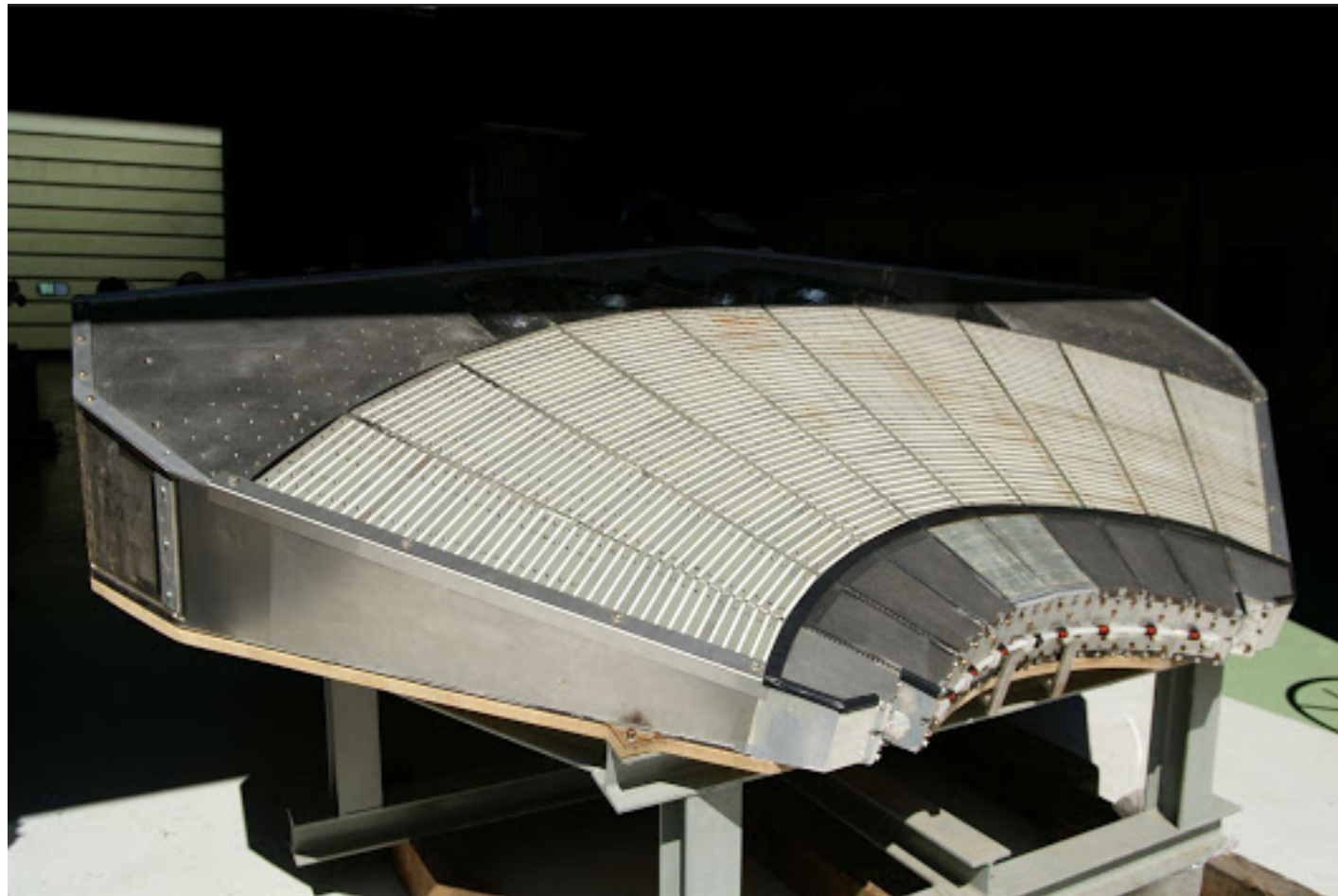
LKr electrode structure (one fourth of the detector is shown)

Examples for sampling calorimeters

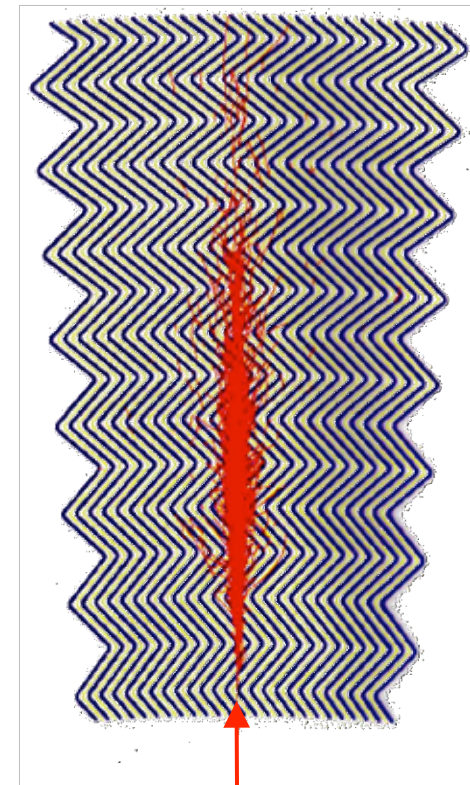
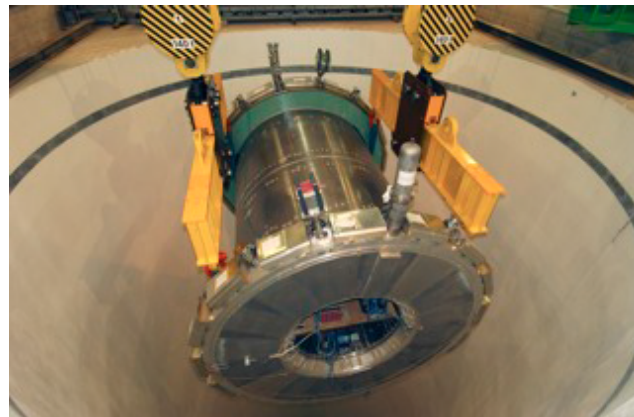
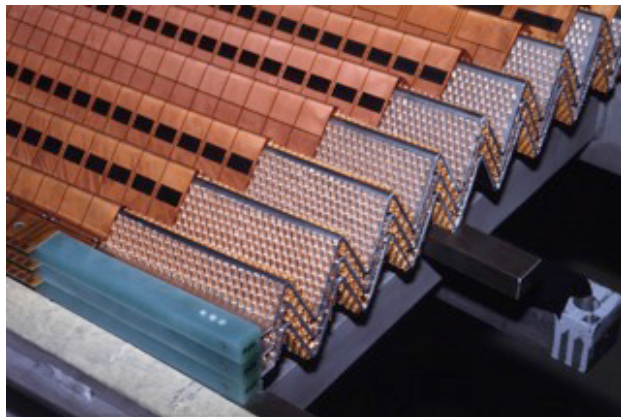
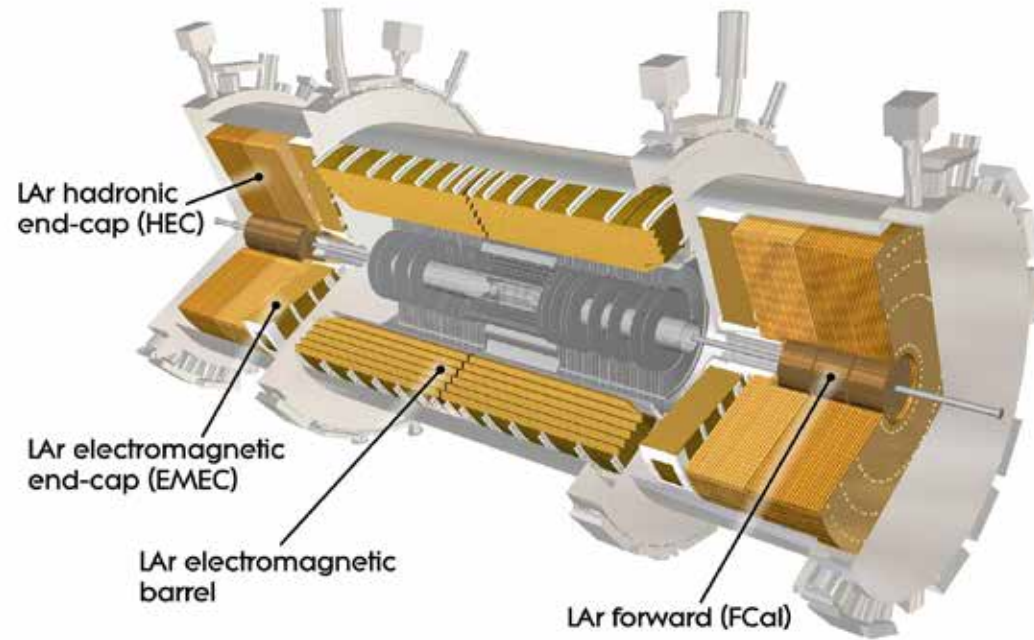


- (a) Scintillators, optically coupled to photomultipliers
- (b) Scintillators, wave length shifters, light guides
- (c) Ionization charge in liquids
- (d) Ionization charge in multi-wire proportional chambers

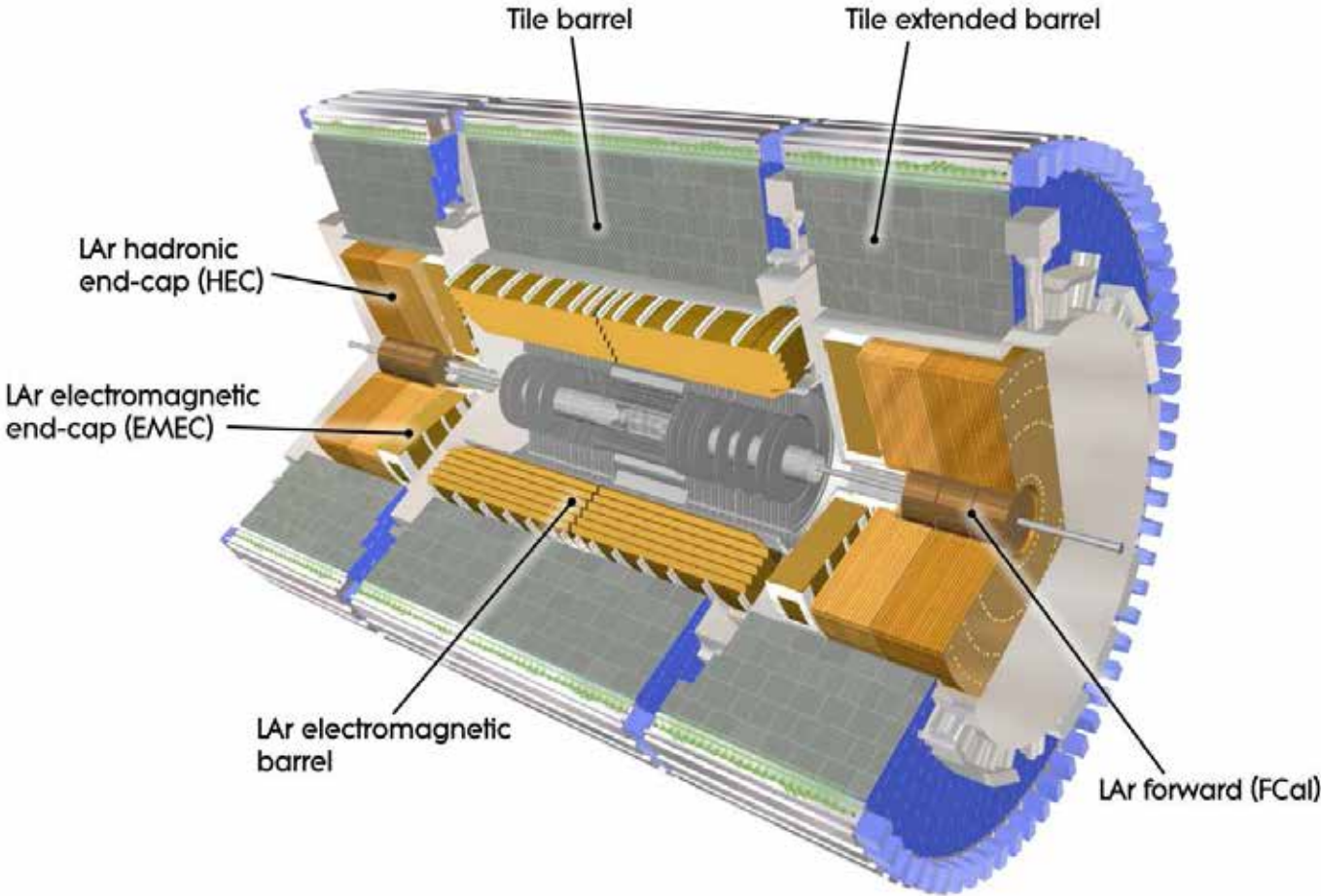
Example: UA2 Lead-scintillator (em) and Fe-scintillator (hadronic) calorimeter



Example: ATLAS Liquid Argon Calorimeter

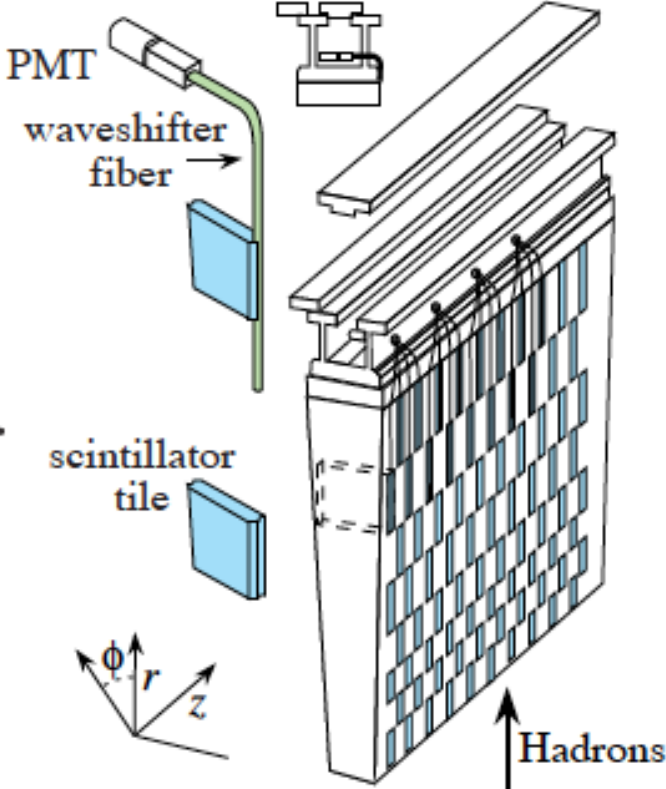
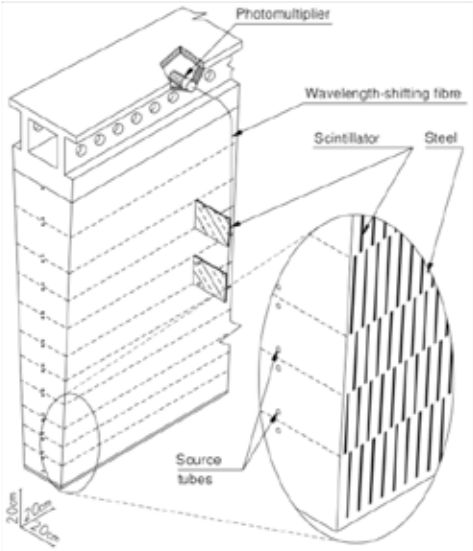
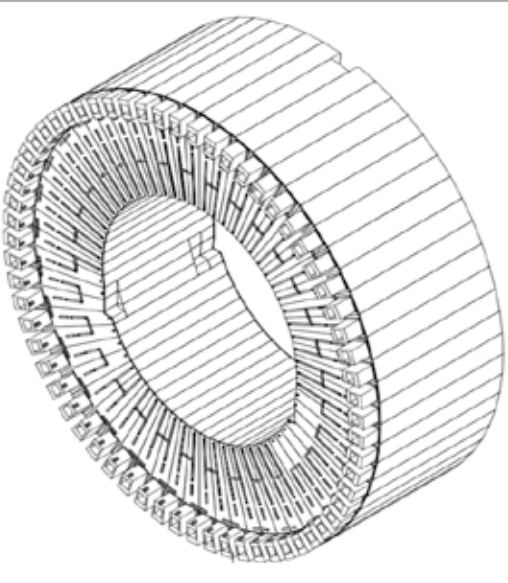


Example: ATLAS Hadronic Tile Calorimeter



Example: ATLAS Hadronic Tile Calorimeter

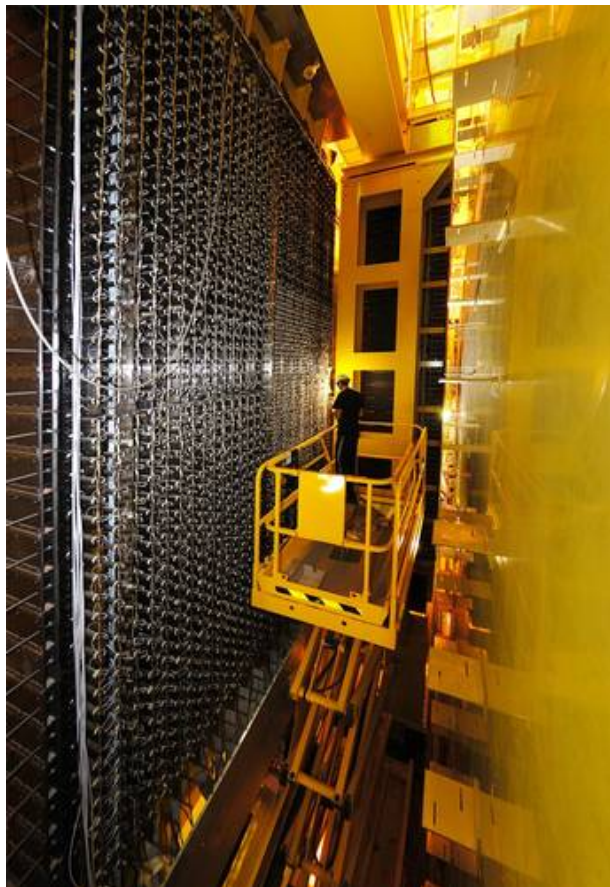
- Iron plates (absorber) interleaved with
- Scintillating tiles



Example: ATLAS Hadronic Tile Calorimeter

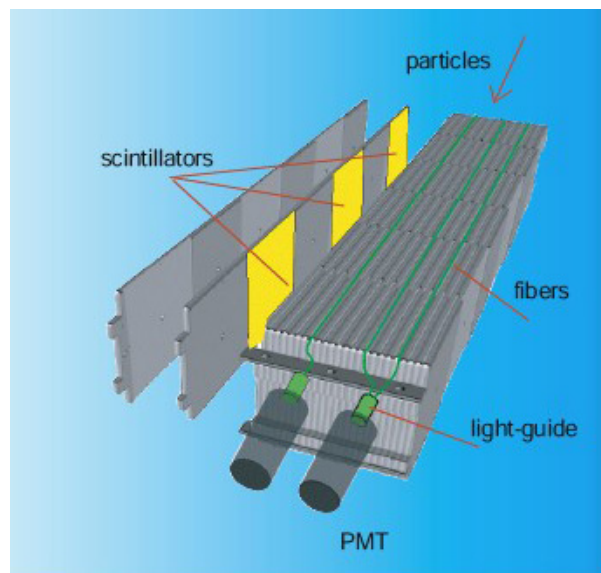


Example: LHCb Hadronic Calorimeter

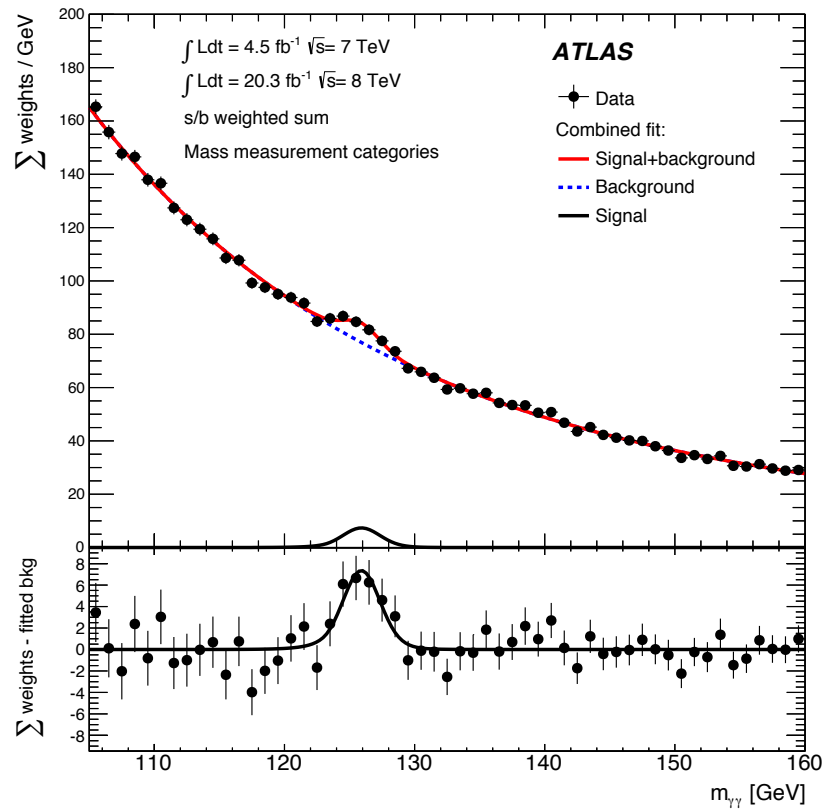


- Iron plates (absorber) interleaved with
- Scintillating tiles

- Arranged parallel to the beam pipe
cell structure: $13 \times 13 \text{ cm}^2$ (inner part), $26 \times 26 \text{ cm}^2$ (outer part)



8.5 Energy resolution of calorimeters



.. the importance of a good calorimeter energy resolution should be clear from this plot

8.5.1 Energy resolution for electromagnetic calorimeters

- The energy resolution of calorimeters depends on the **fluctuations of the measured signal** (for the same energy E_0),
 i.e. on the fluctuation of the measured signal delivered by charged particles, and thereby essentially on their track length (and momentum) in the sensitive medium

- Several effects / fluctuations contribute to the energy resolution:

Homogeneous Calorimeters:

Shower fluctuation	$\sim 1/\sqrt{E}$
Photo-electron statistics	$\sim 1/\sqrt{E}$
Shower leakage	$\approx \text{const}$
Instrumental effects (noise, light attenuation, non-uniformity)	

Sampling calorimeters (in addition):

Sampling fluctuations	$\sim 1/\sqrt{E}$
Landau fluctuations	$\sim 1/\sqrt{E}$
Track length fluctuations	$\sim 1/\sqrt{E}$

- The resolution can be parametrized as:

$$\frac{\Delta E}{E} = \frac{\alpha}{\sqrt{E}} \oplus \beta \oplus \frac{\gamma}{E}$$

α is the so called **stochastic term** (statistical fluctuations)

β is the **constant term** (dominates at high energies)

γ is the **noise term** (electronic noise,..)

(i) Shower fluctuations

For an ideal (homogeneous) calorimeter without losses (quantum efficiency, cutoffs, ...) the energy resolution is limited only by the statistical fluctuations of the number N of shower particles

On average: $N = E_0 / W$ signal carriers (e.g. e-ion pairs in liquids) are produced

with: E_0 = energy of the primary particle

W = mean energy to produce a "signal quantum" (e, light)

(Silicon: $W = 3.6$ eV, Gases: $W \approx 30$ eV, Plastic scintillators: $W \approx 100$ eV)

The fluctuations on N result in a fluctuation in the energy resolution:

$$\frac{\Delta E}{E} \propto \frac{\sqrt{N}}{N} = \frac{\alpha}{\sqrt{E}}$$

(ii) Photo-electron Statistics

For detectors for which the deposited energy is measured via light detection, inefficiencies converting photons into a detectable electrical signal (e.g. photo electrons) contribute to the measurement uncertainty. Due to its statistical nature it also scales as $1 / \sqrt{E}$

$$\frac{\Delta E}{E} \propto \frac{\sqrt{N}}{N} = \frac{\alpha}{\sqrt{E}}$$

N_{pe} : number of photo electrons

This contribution is present for calorimeters based on detecting scintillation or Cherenkov light; Important in this context are quantum efficiency and gain of the photo detectors (e.g. photo multipliers, or APDs)

Also losses in light guides and wavelength shifters contribute

(iii) Shower leakage

Due to the finite size of the calorimeters, showers may not be fully contained and there might be leakage

[longitudinally (out of calorimeter) or laterally (e.g. out of defined cluster size)]

Fluctuations in the leakage (e.g. fluctuation in the start of the hadronic shower, first interaction), or in general, fluctuations in free path length before the next interaction degrade the energy resolution

Lateral leakage: limited influence

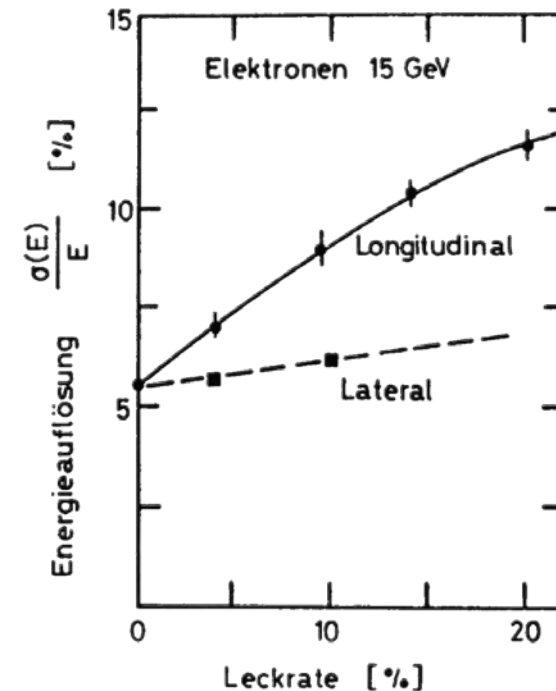
Longitudinal leakage: stronger impact

Typical parametrization to account for leakage effects:
(not unique, other parametrizations exist)

$$\frac{\sigma_E}{E} \propto \left(\frac{\sigma_E}{E} \right)_{f=0} \cdot [1 + 2f\sqrt{E}]$$

[f : average fraction of shower leakage]

→ adds to the constant term in the energy resolution



Degradation of the energy resolution due to lateral and longitudinal leakage (Marble sampling calorimeter, CHARM collaboration, CERN)

(iv) Sampling fluctuations

- In sampling calorimeters, an additional contribution to the energy resolution results from fluctuations in the number of (low-energy) electrons crossing the active / sensitive layer
- This number depends on the incident particle energy and is found to be inversely proportional to the thickness of the passive layer

$$N_{\text{ch}} \propto \frac{E}{E_c t_{\text{abs}}}$$

N_{ch} : charged particles reaching active layer
 N_{max} : total number of particles = E/E_c
 t_{abs} : absorber thickness in X_0

Reasoning: Energy deposition in the active layers is dominated by low energy particles (electrons, pions), the probability that they reach the active layer and are not absorbed in the passive material increases for thinner passive layers

→ The resulting contribution to the energy resolution can be parametrized as:

$$\frac{\sigma_E}{E} \propto \frac{\sigma_{N_{\text{ch}}}}{N_{\text{ch}}} \propto \sqrt{\frac{E_c t_{\text{abs}}}{E}}$$

Semi-empirical:

$$\frac{\sigma_E}{E} = 3.2\% \sqrt{\frac{E_c [\text{MeV}] \cdot t_{\text{abs}}}{F \cdot E [\text{GeV}]}}$$

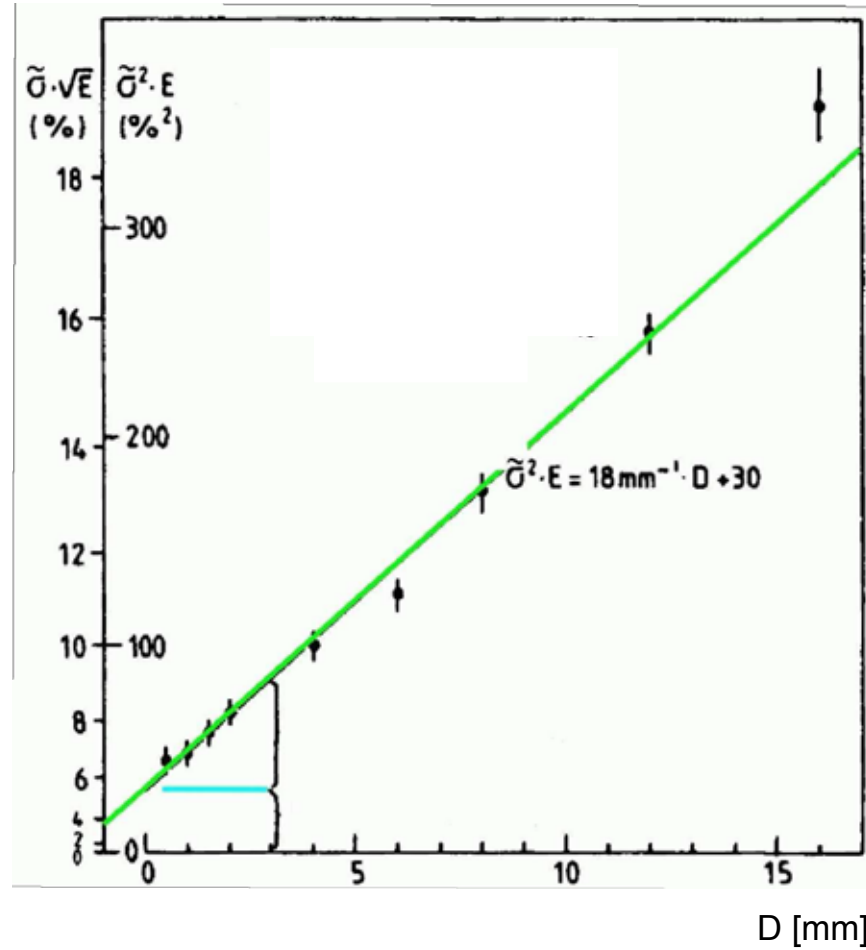
→ Finer samplings (thin passive layers) preferred (sampling fraction is obviously increased)

where F takes detector threshold effects into account ...

Measured energy resolution of a sampling calorimeter as a function of the absorber thickness D

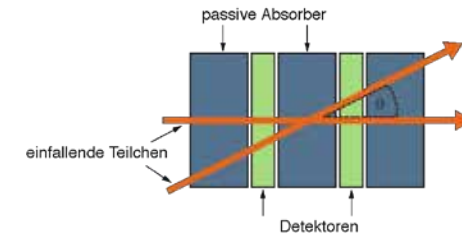
Sampling contribution:

$$\frac{\sigma_E}{E} = 3.2\% \sqrt{\frac{E_c[\text{MeV}] \cdot t_{\text{abs}}}{F \cdot E[\text{GeV}]}}$$



(v) Track lengths fluctuations

- Due to multiple scattering, particles in the shower transverse the absorber under different angles
→ different effective absorber thickness $t_{\text{abs}} \rightarrow t_{\text{abs}} / \cos \theta$



Due to the narrowness of electromagnetic showers, this effect is small

(vi) Landau fluctuations

- The asymptotic energy loss distribution (dE/dx) for thin active layers yields corrections (Landau instead of Gaussian distribution)

$$\frac{\sigma_E}{E} = \frac{1}{\sqrt{N_{\text{ch}}}} \cdot \frac{3}{\ln(k \cdot \delta)}$$

[semi-empirical]

with:

- k : constant; $k = 1.3 \cdot 10^4$ if δ measured in MeV
- δ : average energy loss in active layer ('thickness')

→ thin active layers are disfavoured

Examples for energy resolutions seen in electromagnetic calorimeters in large detector systems:

Experiment	Calorimeter	α	β	γ	
L3	BGO	2.0%	0.7%		homogeneous calorimeters
BaBar	CsI (TI)	(*) 2.3%	1.4%	40 MeV	
CMS	PbWO ₄	3.0%	0.5%	200 MeV	
OPAL	Lead glass	(**) 5% (++) 3%			
NA48	Liquid krypton	3.2%	0.4%	90 MeV	sampling calorimeters
UA2	Pb / Scintillator	15%	1.0%		
ALEPH	Pb / Prop. chambers	18%	0.9%		
ZEUS	U / Scintillator	18%	1.0%		
H1	Pb / Liquid argon	12.0%	1.0%	150 MeV	
D0	U / Liquid argon	16.0%	0.3%	300 MeV	
ATLAS	Pb / Liquid argon	10.0%	0.4%	200 MeV	

(*) scaling according to $E^{-1/4}$ rather than $E^{-1/2}$

(**) at 10 GeV

(++) at 45 GeV

Technology (Experiment)	Depth	Energy resolution	Date
NaI(Tl) (Crystal Ball)	$20X_0$	$2.7\%/E^{1/4}$	1983
Bi ₄ Ge ₃ O ₁₂ (BGO) (L3)	$22X_0$	$2\%/ \sqrt{E} \oplus 0.7\%$	1993
CsI (KTeV)	$27X_0$	$2\%/ \sqrt{E} \oplus 0.45\%$	1996
CsI(Tl) (BaBar)	$16-18X_0$	$2.3\%/E^{1/4} \oplus 1.4\%$	1999
CsI(Tl) (BELLE)	$16X_0$	1.7% for $E_\gamma > 3.5$ GeV	1998
PbWO ₄ (PWO) (CMS)	$25X_0$	$3\%/ \sqrt{E} \oplus 0.5\% \oplus 0.2/E$	1997
Lead glass (OPAL)	$20.5X_0$	$5\%/ \sqrt{E}$	1990
Liquid Kr (NA48)	$27X_0$	$3.2\%/ \sqrt{E} \oplus 0.42\% \oplus 0.09/E$	1998
Scintillator/depleted U (ZEUS)	$20-30X_0$	$18\%/ \sqrt{E}$	1988
Scintillator/Pb (CDF)	$18X_0$	$13.5\%/ \sqrt{E}$	1988
Scintillator fiber/Pb spaghetti (KLOE)	$15X_0$	$5.7\%/ \sqrt{E} \oplus 0.6\%$	1995
Liquid Ar/Pb (NA31)	$27X_0$	$7.5\%/ \sqrt{E} \oplus 0.5\% \oplus 0.1/E$	1988
Liquid Ar/Pb (SLD)	$21X_0$	$8\%/ \sqrt{E}$	1993
Liquid Ar/Pb (H1)	$20-30X_0$	$12\%/ \sqrt{E} \oplus 1\%$	1998
Liquid Ar/depl. U (DØ)	$20.5X_0$	$16\%/ \sqrt{E} \oplus 0.3\% \oplus 0.3/E$	1993
Liquid Ar/Pb accordion (ATLAS)	$25X_0$	$10\%/ \sqrt{E} \oplus 0.4\% \oplus 0.3/E$	1996

8.5.2 Energy resolution for hadronic calorimeters

The energy resolution of hadronic calorimeter can as well be parametrized with the canonical formula, however, the coefficients α , β , and γ are significantly larger;

Typical values: α : 35 – 100%, β : 3 – 5%, γ : 1-3 GeV

The contributions are listed below (additional ones are marked in red)

$$\frac{\Delta E}{E} = \frac{\alpha}{\sqrt{E}} \oplus \beta \oplus \frac{\gamma}{E}$$

Shower fluctuations
Sampling fluctuations *)
Leakage fluctuations
Photo-electron statistics (if relevant)
Track length and Landau fluctuations
Fluctuations of the electromagnetic fraction
Fluctuations in the neutron component
Fluctuations in the invisible energy
Fluctuations in binding energy losses
Fluctuations in nuclear excitation, fission, ...
Fluctuations in the number of heavily ionizing particles

Shower leakage
Inhomogeneities
Calibration
Hadron / electron response
Electronic noise

*) Due to the many intrinsic effects of hadronic showers, the relative importance of the sampling fluctuations is much lower in hadronic calorimeters

Examples for energy resolutions seen in hadronic calorimeters in large detector systems:

Experiment	Calorimeter	α	β	γ
ALEPH	Fe /Streamer tubes	85%		
ZEUS (*)	U / Scintillator	35%	2.0%	
H1 (**)	Fe / Liquid argon	51%	1.6%	0.9 GeV
D0	U / Liquid argon	41%	3.2%	1.4 GeV

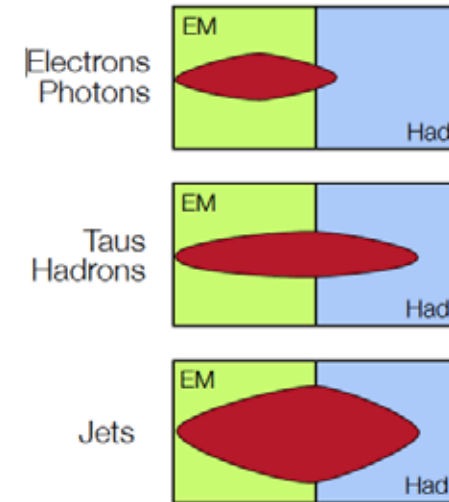
(*) Compensating calorimeter

(**) Weighting technique

The measurement of hadron / jet energies extends over both the **electromagnetic and the hadronic calorimeter**

→ inter-calibration between the two calorimeters is needed;

non-trivial due to different layouts / sensitive media



Observed Features of Hadronic Calorimeter Measurements

Requirements (ideal):

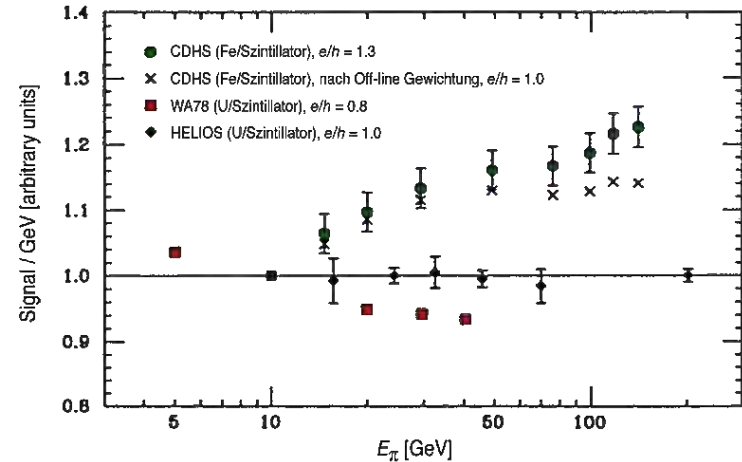
- Linear response: $S \sim E$
- Independent of particle type
- Gaussian distributions,
- resolution scaling as $1/\sqrt{E}$

Reality:

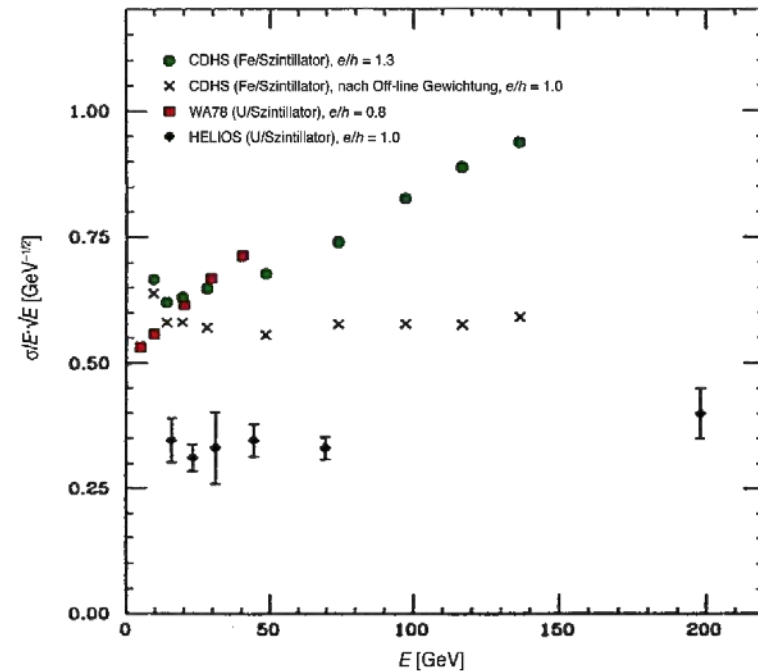
- (i) Non-linear response
- (ii) e/h ratio differs from 1
- (iii) Non-Gaussian tails
- (iv) Deviations from $1/\sqrt{E}$ scaling

Data suggest that $e/h = 1$ is beneficial for both linearity of response and scaling of resolution

Response, as measured for various hadron calorimeters



Deviations from $1/\sqrt{E}$ scaling of the resolution



e/h ratio

In general the response of calorimeters is different for electromagnetic and hadronic showers

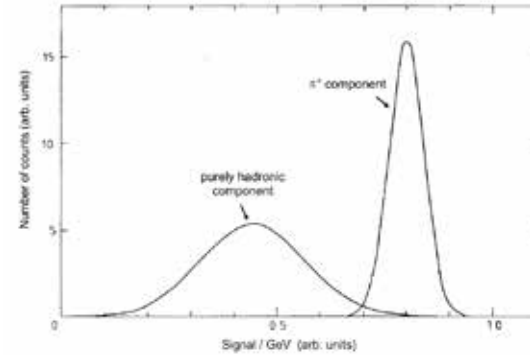
Usually higher response to electromagnetic showers
→ $e/h > 1$

$e/h \neq 1$ leads to non-uniform response, due to varying electromagnetic fraction f_{em} ,
 $f_{em} \sim \ln(E)$

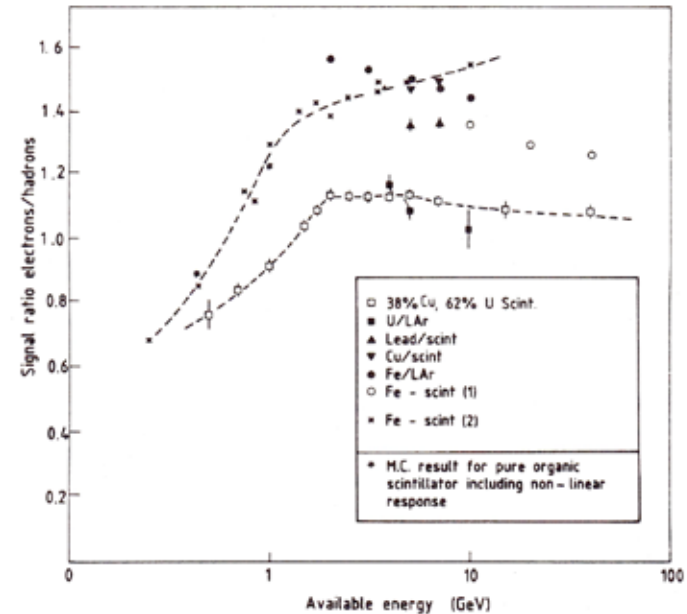
Fluctuations in $f_{em} \rightarrow$ non-Gaussian tails in resolution

→ compensation, i.e. $e/h = 1$, is important

Response to π^0 and hadron component



Measured ratios of e/h response as function of the particle energy



e/h ratio

In general the response of calorimeters is different for electromagnetic and hadronic showers

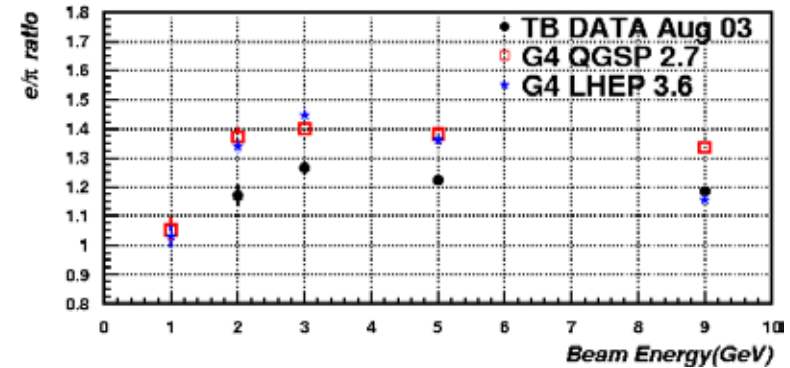
Usually higher response to electromagnetic showers
→ $e/h > 1$

$e/h \neq 1$ leads to non-uniform response, due to varying electromagnetic fraction f_{em} ,
 $f_{em} \sim \ln(E)$

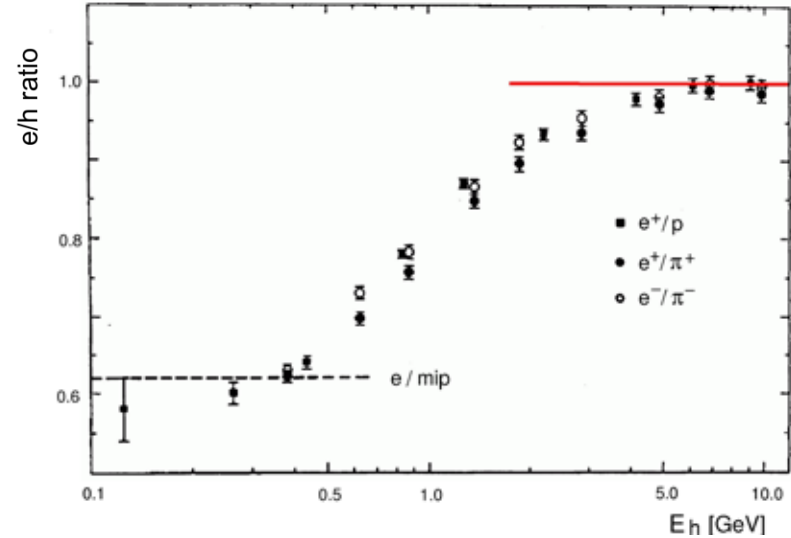
Fluctuations in $f_{em} \rightarrow$ non-Gaussian tails in resolution

→ compensation, i.e. $e/h = 1$, is important

e/p as measured in ATLAS tile calorimeter (testbeam)



ZEUS U/scintillator calorimeter shows $e/h = 1$ (down to low energies)



Compensation

Consider particle type i with energy $E(i)$:

$$E_{\text{vis}}(i) = E_{\text{dep}}(i) - E_{\text{inv}}(i)$$

$$a_i \equiv \frac{E_{\text{vis}}(i)}{E_{\text{vis}}(i) + E_{\text{inv}}(i)}$$

E_{vis} : visible energy

E_{dep} : deposited energy

E_{inv} : invisible energy

Visible energy fraction

Compare energy deposition of different particle types with that of minimum ionizing particle (mip):

$$\frac{e}{\text{mip}} = \frac{a_e}{a_{\text{mip}}} \quad \text{[Electromagnetic component]}$$

$$\frac{h}{\text{mip}} = \frac{a_h}{a_{\text{mip}}} \quad \text{[Hadronic components]}$$

detector signal

determined by calibration

$$S_e = k \cdot E \frac{e}{\text{mip}} \quad \text{[Electron signal]}$$

$$S_h = k \cdot E \left[f_{\text{em}} \frac{e}{\text{mip}} + (1 - f_{\text{em}}) \frac{h}{\text{mip}} \right] \quad \text{[Hadronic signal]}$$

electromagn. energy fraction [varies with $\ln E$]

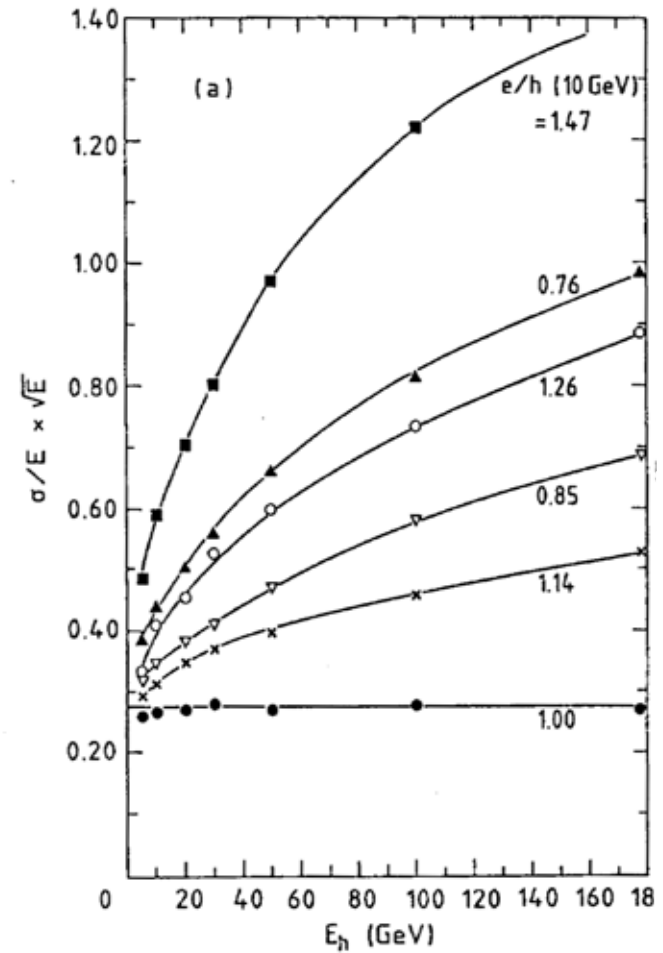
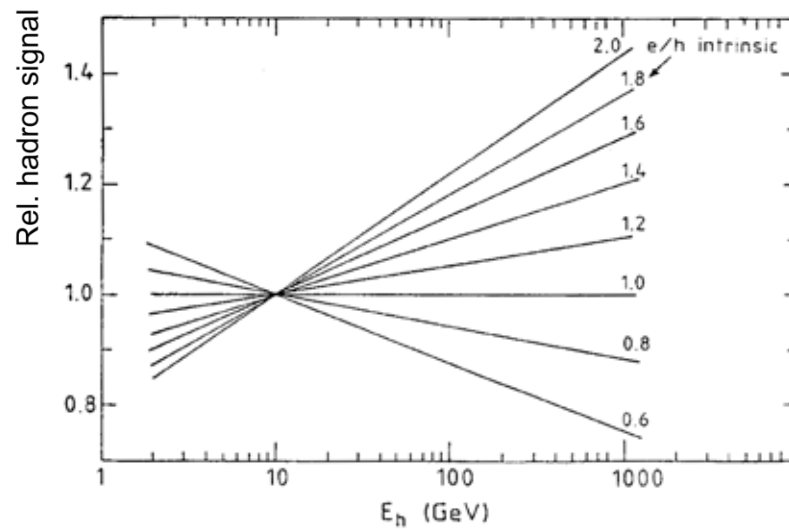
$$\frac{S_e}{S_h} = \frac{\frac{e}{\text{mip}}}{f_{\text{em}} \frac{e}{\text{mip}} + (1 - f_{\text{em}}) \frac{h}{\text{mip}}}$$

mip = muon
(proper normalization, standard candle)

Consequences of non-compensation:

a) Hadron signals get larger (smaller) with E_h
if $e/h > 1$ ($e/h < 1$)

b) Energy resolution does not scale as $1/\sqrt{E}$
for $e/h \neq 1$



Contributions to h/mip :

$$\frac{h}{mip} = f_{ion} \cdot \frac{ion}{mip} + f_n \cdot \frac{n}{mip} + f_\gamma \cdot \frac{\gamma}{mip} + f_B \cdot \frac{B}{mip}$$

with:

f_{ion} : fraction of hadronic component deposited by charged particles (ionization)

f_n : fraction of hadronic component deposited by neutrons

f_γ : fraction of hadronic component deposited by photons from nuclear reactions

f_B : fraction of nuclear binding energy in hadronic component

Compensation:

Increase h/mip via increase

of $f_{ion}, f_n, f_\gamma, f_B$

	Fe	U		Fe/Sz	Fe/Ar	U/Sz	U/Ar	determined by
f_{ion}	57%	38%	ion/mip	0.83	0.88	0.93	1	d_{act}
f_n	3%	2%	n/mip	0.5 ... 2	0	0.8 ... 2.5	0	d_{act}/d_{abs}
f_γ	8%	15%	γ /mip	0.7	0.95	0.4	0.4	d_{abs}
f_B	32%	45%	B/mip	0.9	0.95	0.55	0.55	d_{abs}

d_{act} : thickness of active medium
 d_{abs} : thickness of absorber

Contributions to h/mip :

$$\frac{h}{mip} = f_{ion} \cdot \frac{ion}{mip} + f_n \cdot \frac{n}{mip} + f_\gamma \cdot \frac{\gamma}{mip} + f_B \cdot \frac{B}{mip}$$

with:

f_{ion} : fraction of hadronic component deposited by charged particles (ionization)

f_n : fraction of hadronic component deposited by neutrons

f_γ : fraction of hadronic component deposited by photons from nuclear reactions

f_B : fraction of nuclear binding energy in hadronic component

Compensation:

Increase h/mip via increase

of $f_{ion}, f_n, f_\gamma, f_B$

Methods to achieve compensation:

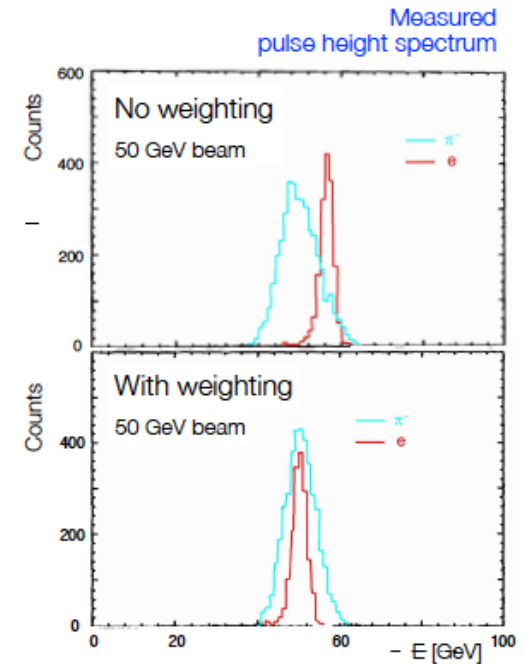
- (i) Weighting techniques in calorimeters with high granularity
Try to identify el.magn. sub-showers
- (ii) Optimize hardware / calorimeter layout to boost hadronic response
(i.e. work on the terms given above)

(i) *Weighting Techniques (software compensation)*

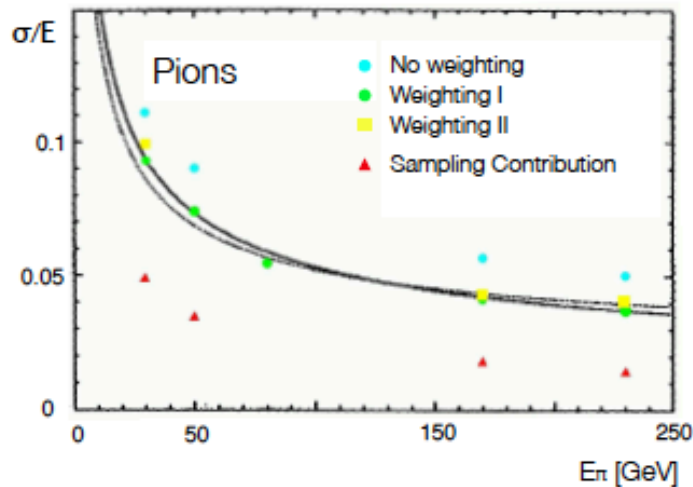
- Identify cells with a high energy density

The corresponding energy deposition is likely to come from an electromagnetically interacting particle ($\pi^0 \rightarrow \gamma\gamma$)

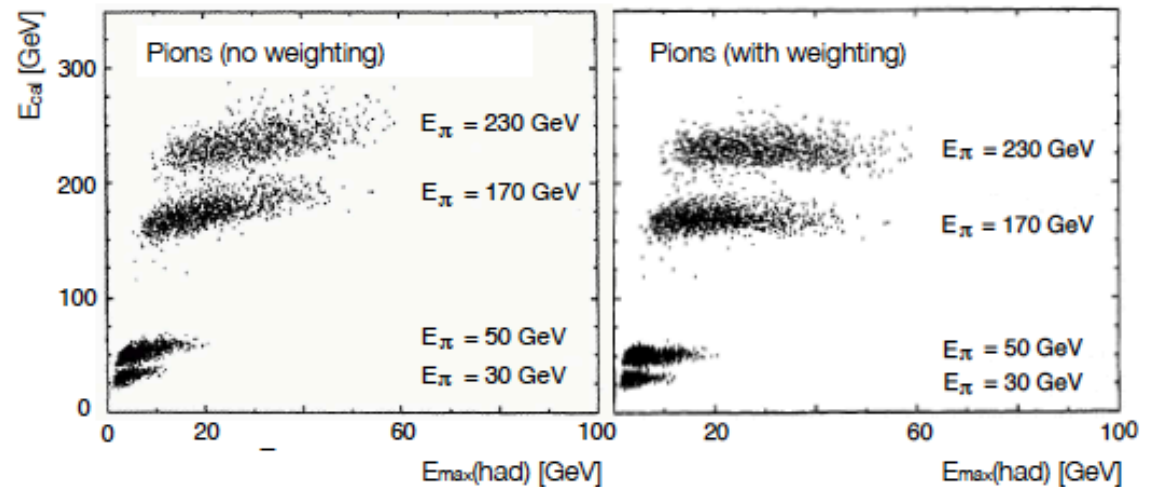
→ weight it down to lower the e.m. response within the hadronic shower



Energy resolution of LAr calorimeter with and without weighting ...



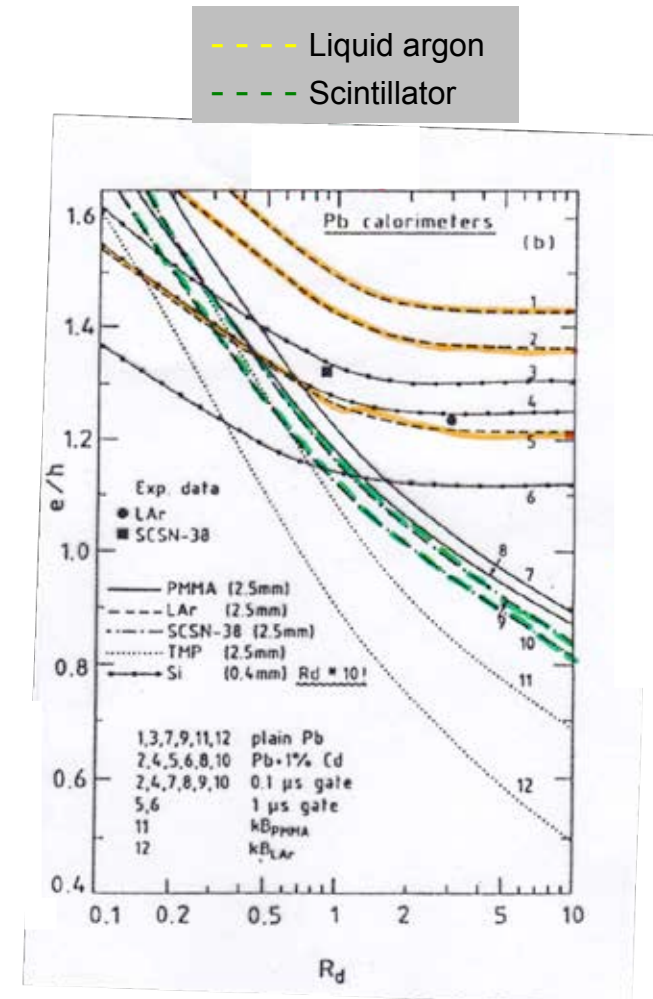
Energy measurement as function of $E_{max}(had)$...



(ii) Hardware compensation

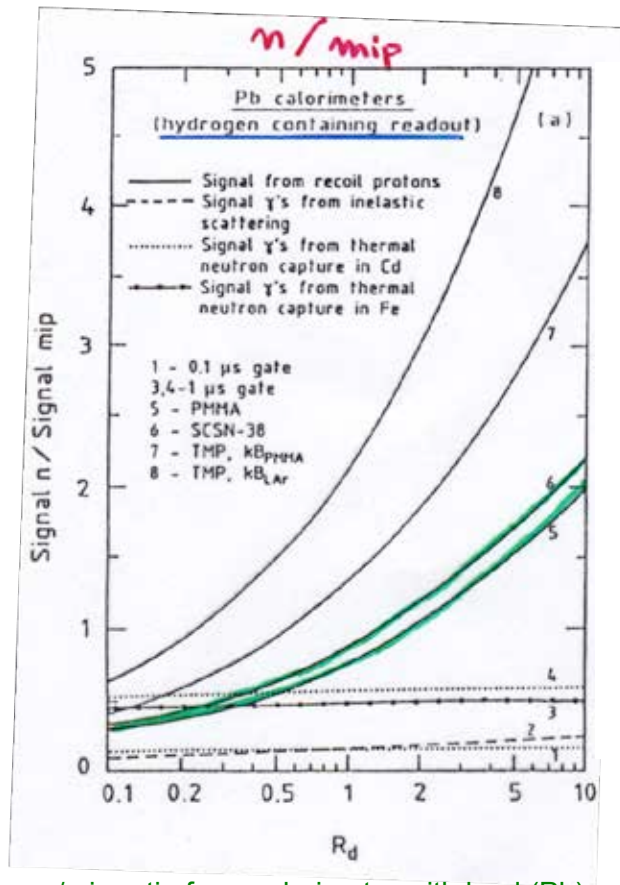
Choose suitable hardware parameters to either increase h/mip or to decrease e/mip :

- Increase the hadronic response by varying the thicknesses of the active and absorber material (d_{abs} and d_{act})
- Increase the hadronic response via fission and spallation of uranium
- Increase the neutron detection efficiency in the active material → use materials with a high proton content, e.g. H_2 (works for scintillators, but not for liquid argon → plot, next page)
- Reduce the e/mip via high-Z absorber and suitable choice of d_{abs} / d_{act} → plot (for Pb sampling calorimeter)
- Increase the integration time for higher sensitivity to (n, γ) -reactions after neutron thermalization
- Modify f_n choosing larger Z_{abs} since the fraction of spallation neutrons increases with Z/A



e/h ratio for a calorimeter with lead (Pb) absorber plates as a function of the ratio of thickness of the absorber to the thickness of the active (sensitive) layers
 $R_d = d_{abs} / d_{act}$ for different sensitive materials

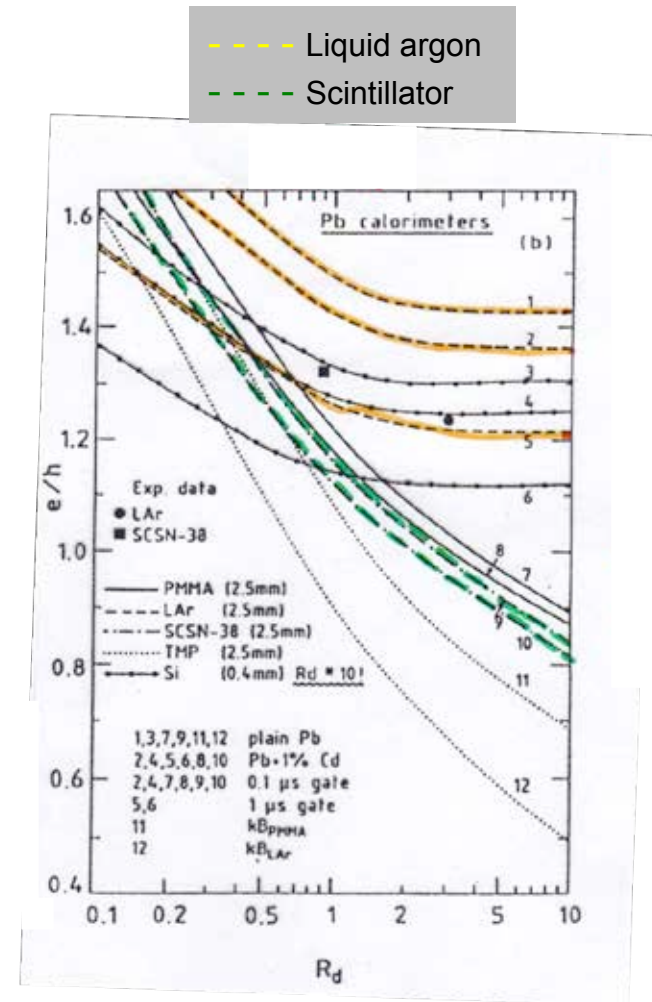
Hardware compensation (cont.)



n/mip ratio for a calorimeter with lead (Pb) absorber plates as a function of the ratio of thickness of the absorber to the thickness of the active (sensitive) layers

$R_d = d_{abs} / d_{act}$ for different sensitive materials

*note: n / mip << 1 in liquid argon (curve 2)



e/h ratio for a calorimeter with lead (Pb) absorber plates as a function of the ratio of thickness of the absorber to the thickness of the active (sensitive) layers

$R_d = d_{abs} / d_{act}$ for different sensitive materials

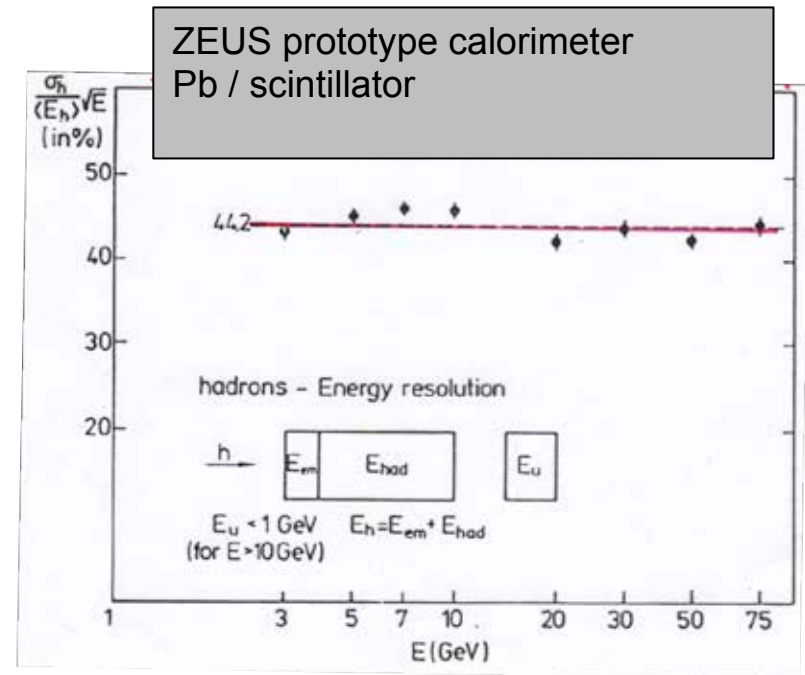
--- Liquid argon
 --- Scintillator

Conclusion on compensation:

Towards the end of 1980s lot of R&D (Research and Development) work on hadron calorimetry was performed (R. Wigmans et al. and ZEUS collaboration)

It was demonstrated that:

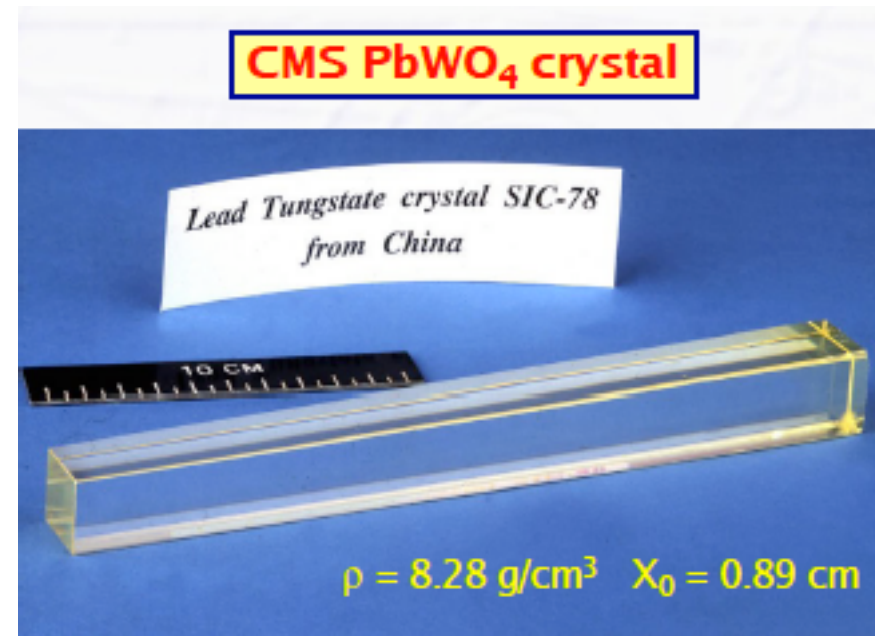
- Compensation can be reached in:
uranium calorimeters
- .or.
- Calorimeters with other high-Z materials if
proper choice of ratio of absorber to active
layer thickness is made
e.g. for Pb absorbers with $R_d \approx 2$
- Compensation in Liquid argon calorimeters
seems only possible for uranium absorbers
(only way to increase n contribution via fission,
unlike via recoil in hydrogen rich materials)



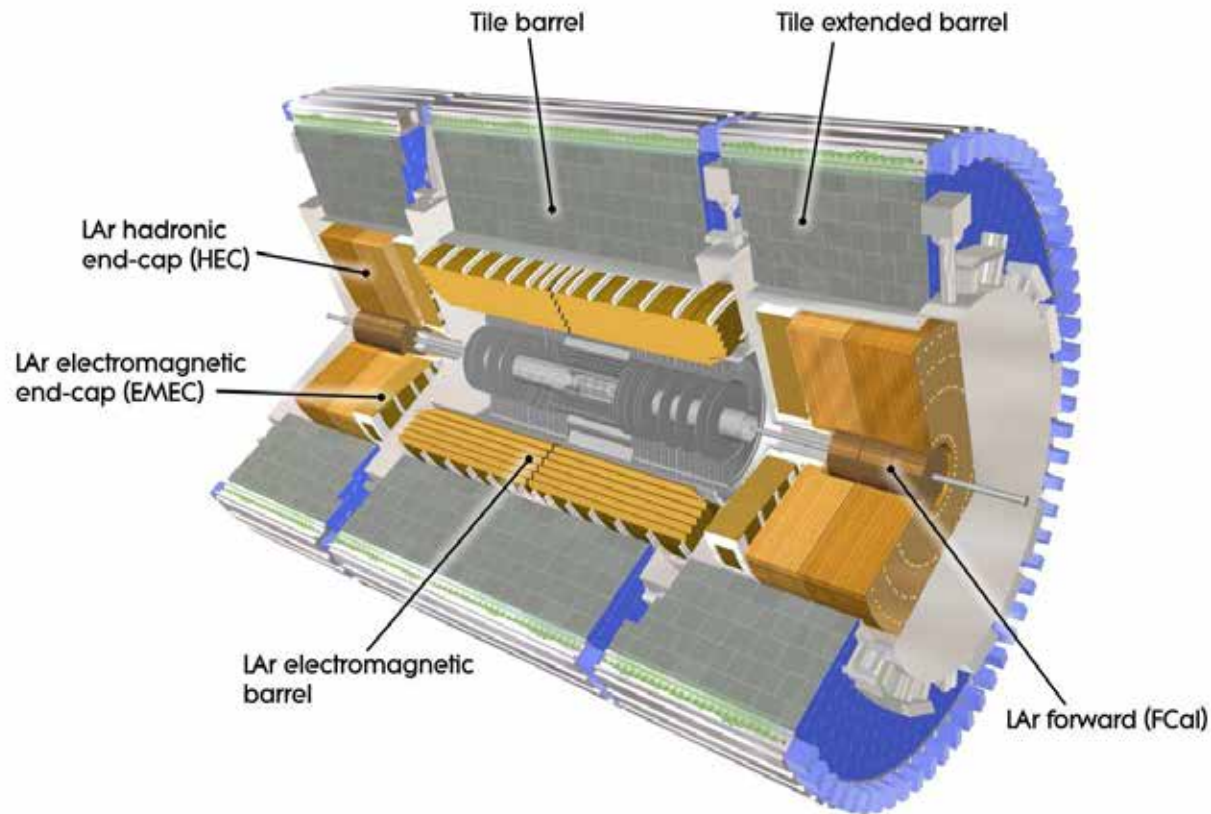
The energy resolution for hadrons vs. the beam energy in a compensating lead/scintillator prototype calorimeter of the ZEUS collaboration

8.6 The ATLAS and CMS

calorimeters



The ATLAS calorimeter system



- Liquid argon electromagnetic
- Liquid argon hadron calorimeter in the end-caps and forwards regions
- Scintillator tile hadron calorimeter in the barrel and extended end-cap region

ATLAS and CMS electromagnetic calorimeters

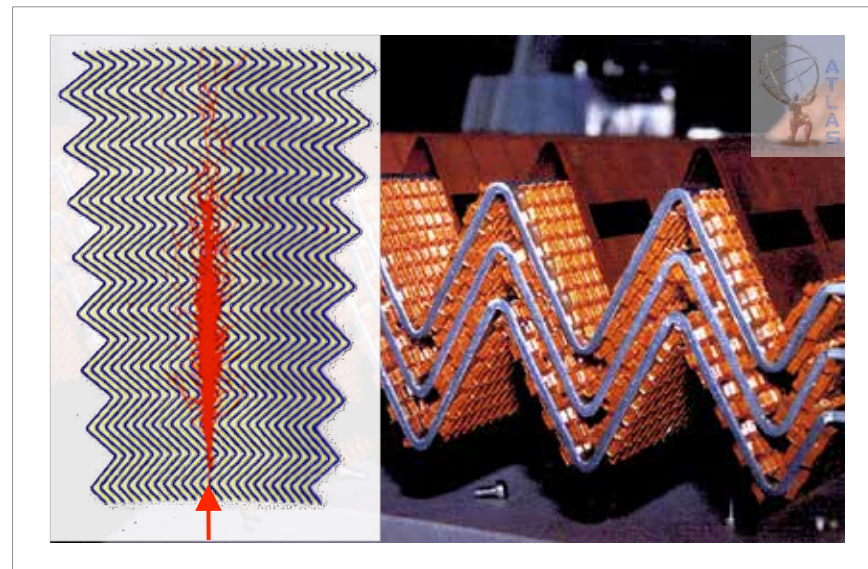
■ CMS: PbWO₄ Scint. Crystal Calorimeter

- Entire shower in active detector material
 - ▶ High density crystals ($28 X_0$)
 - ▶ Transparent, high light yield
 - ▶ No particles lost in passive absorber
 - ▶ High resolution: $\sim 3\%/\sqrt{E}$ (stochastic)
- Granularity
 - ▶ Barrel: $\Delta\eta \times \Delta\phi = 0.017^2$ rad
 - ▶ Longitudinal shower shape unmeasured

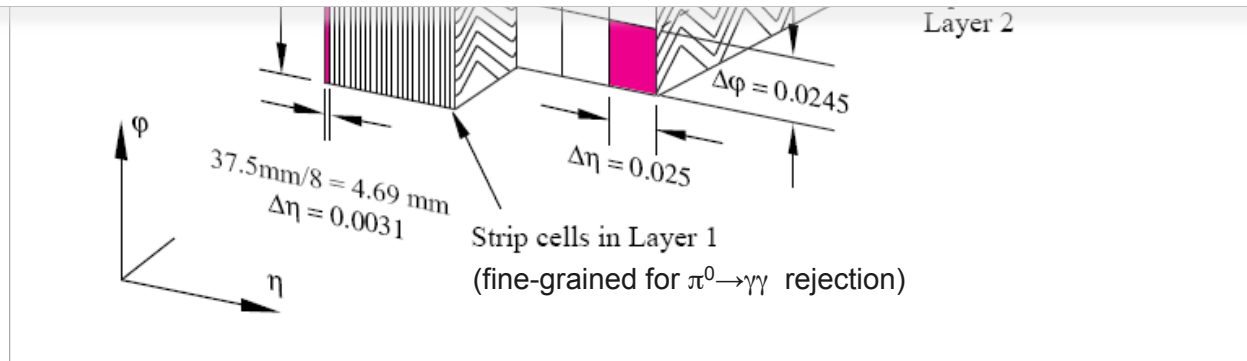
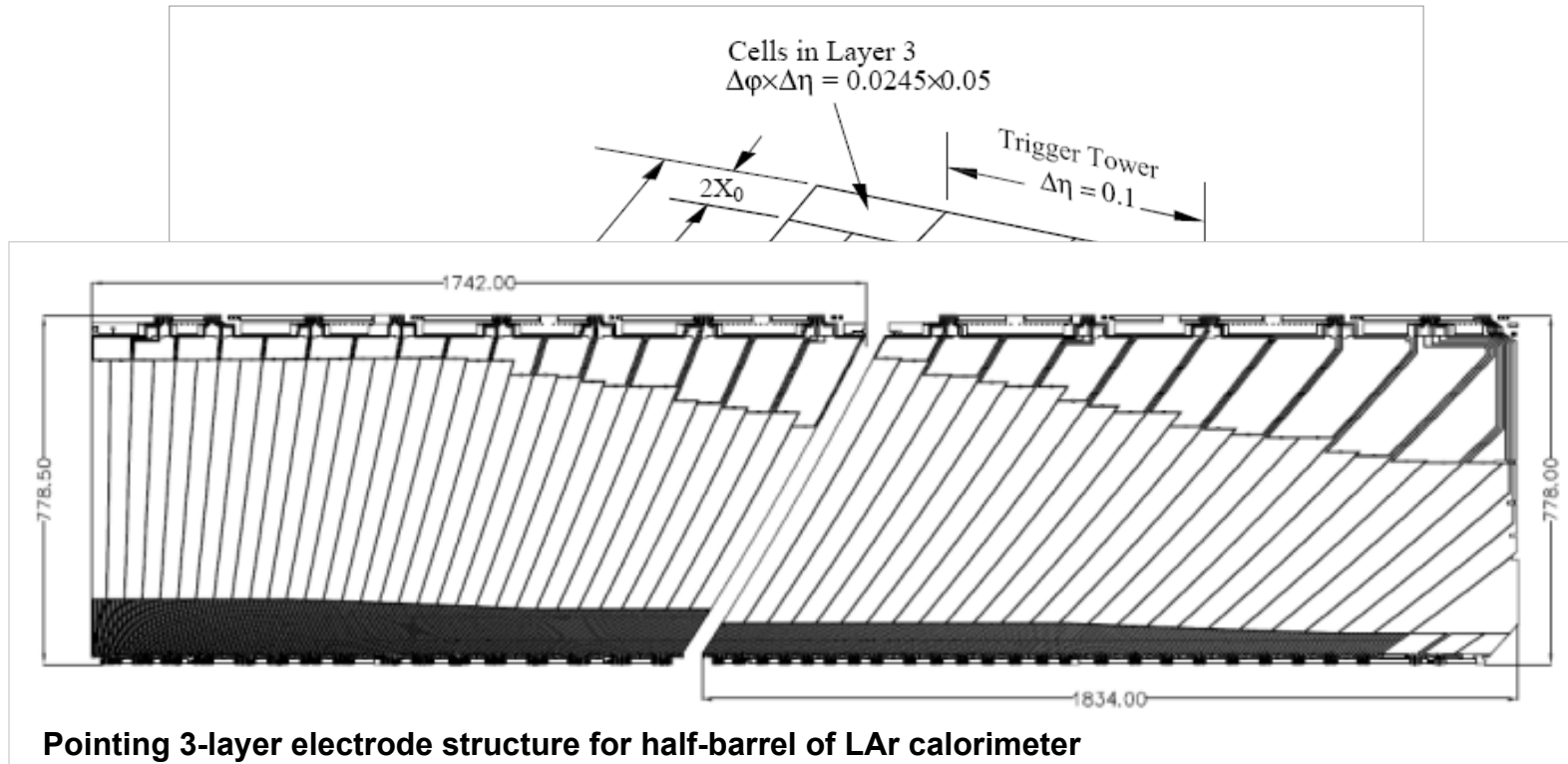


■ ATLAS: LAr Sampling Calorimeter

- Passive, heavy absorber (Pb, 1.1–1.5 mm thick [barrel]) inter-leaved with active detector material (liquid argon)
 - ▶ Overall $22 X_0$
 - ▶ Accordion structure for full ϕ coverage
 - ▶ Resolution: $\sim 10\%/\sqrt{E}$ (stochastic)
- Granularity
 - ▶ Barrel: $\Delta\eta \times \Delta\phi = 0.025^2$ rad (main layer)
 - ▶ Longitudinal segmentation (3 layers)

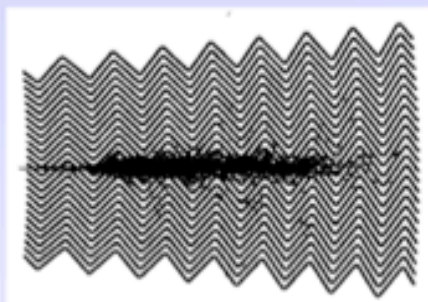


ATLAS Liquid Argon EM Calorimeter



ATLAS electromagnetic Calorimeter

Accordion geometry absorbers immersed in Liquid Argon



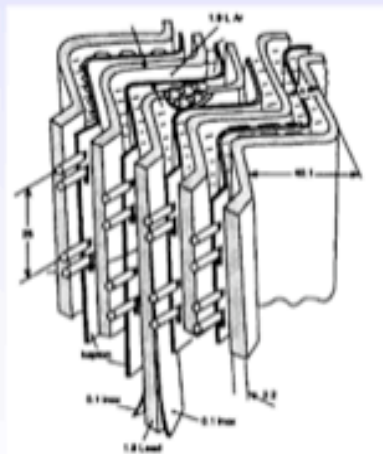
Liquid Argon (90K)

+ lead-steel absorbers (1-2 mm)

+ multilayer copper-polyimide
readout boards

→ Ionization chamber.

1 GeV E-deposit → $5 \times 10^6 e^-$



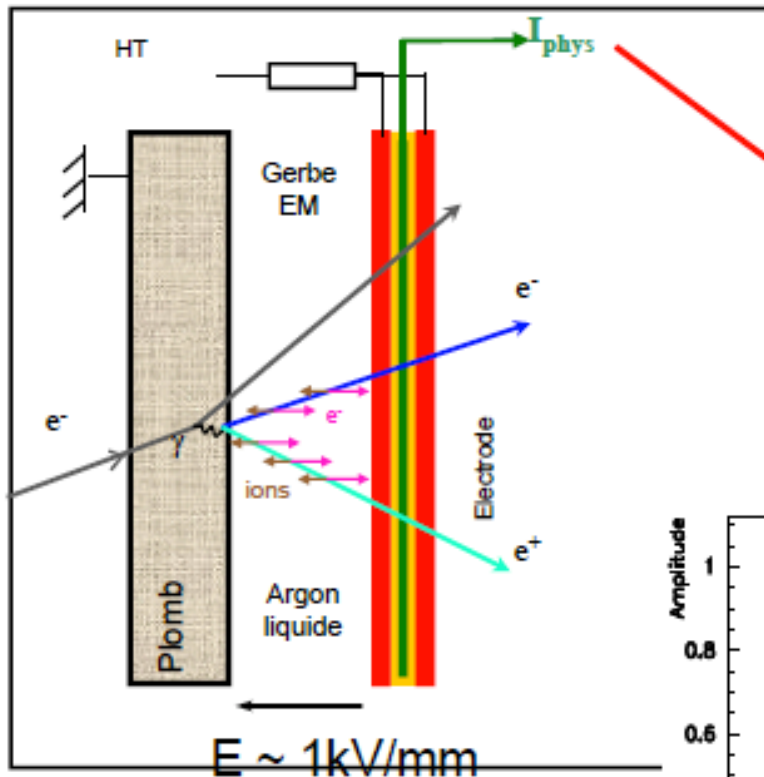
- Accordion geometry minimizes dead zones.
- Liquid Ar is intrinsically radiation hard.
- Readout board allows fine segmentation (azimuth, pseudo-rapidity and longitudinal) acc. to physics needs



Test beam results $\sigma(E)/E = 9.24\%/\sqrt{E} \oplus 0.23\%$

Spatial resolution $\approx 5 \text{ mm} / \sqrt{E}$

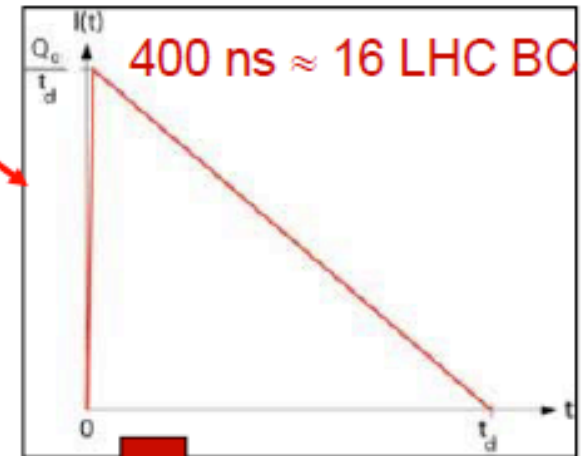
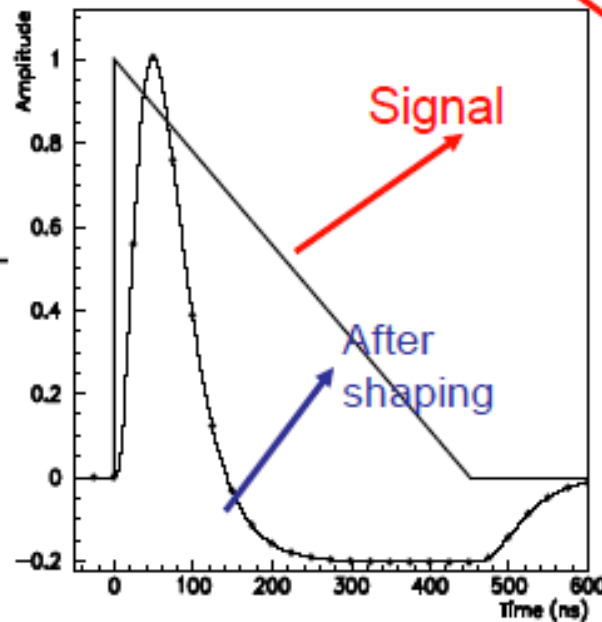
Signal formation in a Liquid argon calorimeter and pulse shaping:



Signal is given from collection of released electrons

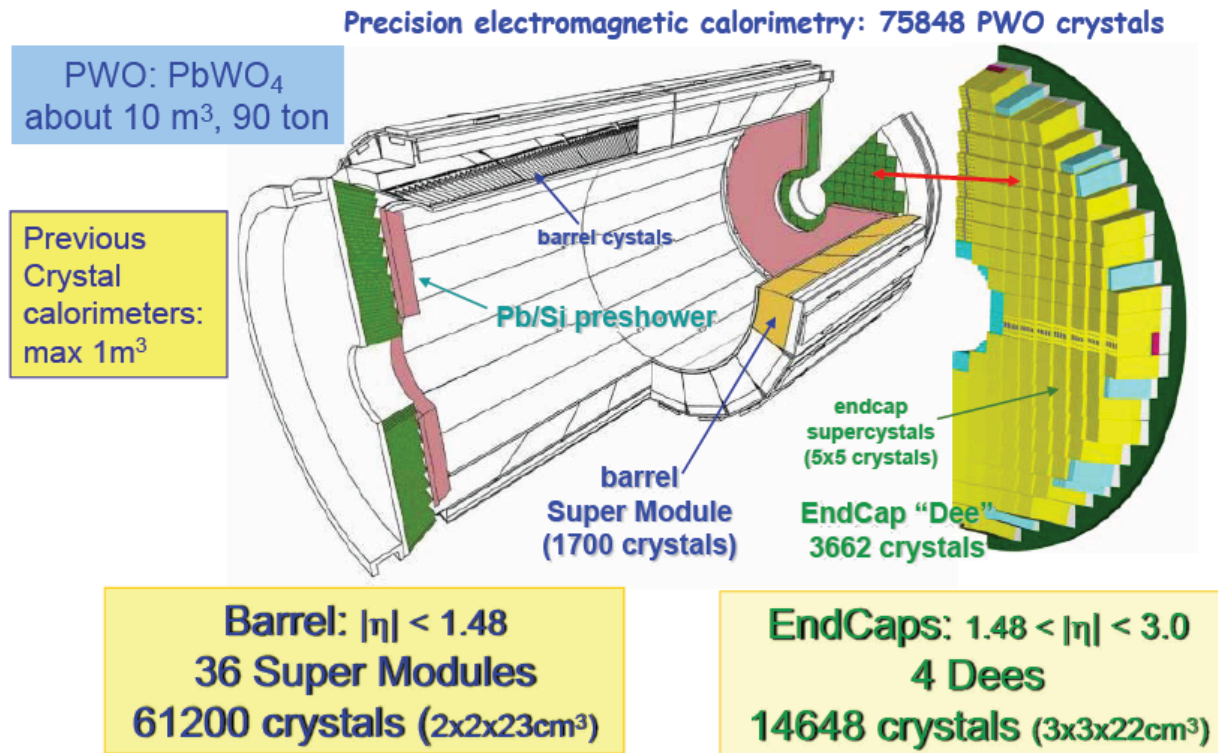
Drift velocity depends on electron mobility and applied field. In ATLAS :

LAr gap 2 mm, $\Delta V = 2\text{kV}$



Instead of total charge (integrated current) measure the initial current I_0 , (via electronic signal shaping), which is also proportional to the energy released

The CMS calorimeter system



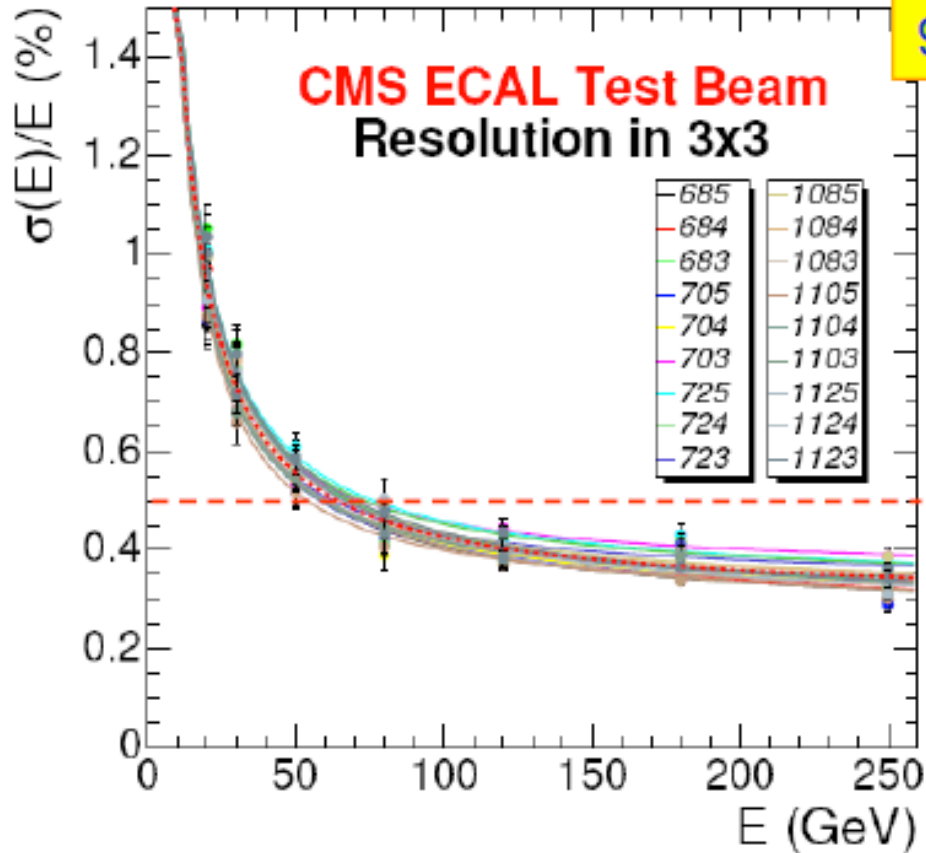
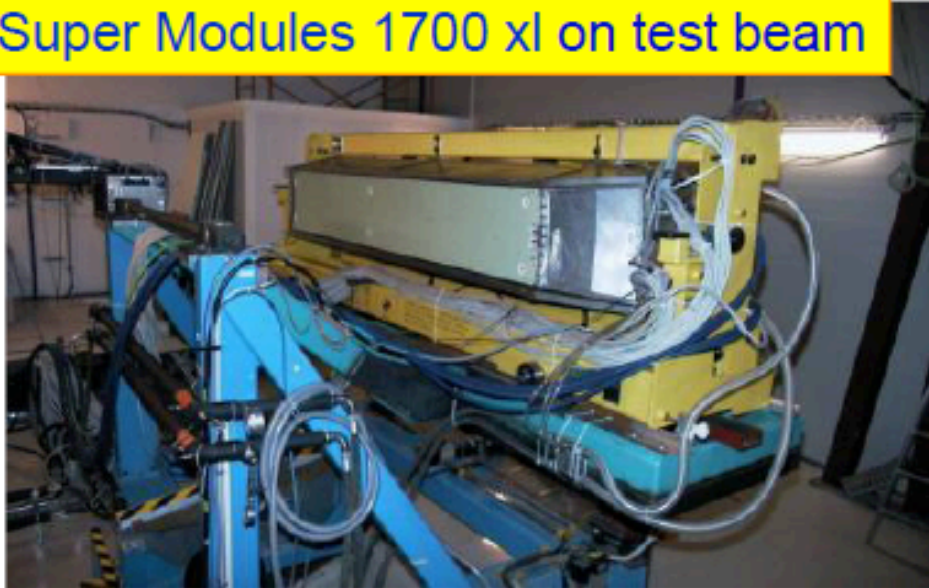
- PbWO_4 crystal
el. magn calorimeter
(homogeneous)
- Hadron calorimeter
integrated in return yoke

CMS el.magnetic calorimeter: crystal PbWO_4

Scintillator	Density [g/cm ³]	X ₀ [cm]	Light Yield γ/MeV (rel. yield*)	τ_1 [ns]	λ_1 [nm]	Rad. Dam. [Gy]	Comments
NaI (Tl)	3.67	2.59	4×10^4	230	415	≥ 10	hygroscopic, fragile
CsI (Tl)	4.51	1.86	5×10^4 (0.49)	1005	565	≥ 10	Slightly hygroscopic
CSI pure	4.51	1.86	4×10^4 (0.04)	10 36	310 310	10^3	Slightly hygroscopic
BaF ₂	4.87	2.03	10^4 (0.13)	0.6 620	220 310	10^5	
BGO	7.13	1.13	8×10^3	300	480	10	
PbWO ₄	8.28	0.89	≈ 100	440 broad band 530 broad band		10^4	light yield =f(T)

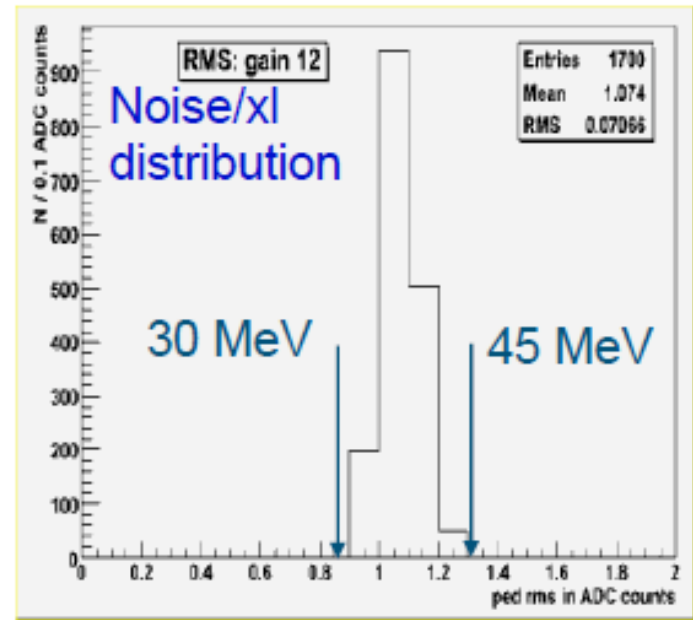


9 Super Modules 1700 xl on test beam



$$\frac{\sigma}{E} = \frac{2.8\%}{\sqrt{E(\text{GeV})}} \oplus \frac{125}{E(\text{MeV})} \oplus 0.3\%$$

Local resolution



Comparison between ATLAS and CMS calorimeters

CMS

Homogeneous calorimeter made of 75000 PbWO_4 scintillating crystals + PS FW

- Very compact $R_M=2.0\text{cm}$
- Excellent energy resolution
- Fast $\ll 100\text{ ns}$
- High granularity
- No longitudinal segmentation
- No angular measurement
- Radiation tolerance : needs follow up
- Room Temperature
- T sensitive $5\%/^\circ\text{K}$
- Requires uniformisation by calibration

ATLAS

Sampling LAr-Pb, 3 Longitudinal layers + PS

- $R_M=7.3\text{cm}$
- Good energy resolution
- Not so fast (450 ns), requires shaping
- High granularity
- Longitudinally segmented
- Angular measurement
- Radiation resistance
- Cryogenic detector (cryostat)
- T sensitive $5\%/^\circ\text{K}$
- Intrinsically uniform

	ATLAS	CMS
EM calorimeter	Liquid argon + Pb absorbers $\sigma/E \approx 10\%/\sqrt{E} + 0.007$	PbWO_4 crystals $\sigma/E \approx 3\%/\sqrt{E} + 0.003$
Hadronic calorimeter	Fe + scintillator / Cu+LAr (10 λ) $\sigma/E \approx 50\%/\sqrt{E} + 0.03\text{ GeV}$	Brass + scintillator (7 λ + catcher) $\sigma/E \approx 100\%/\sqrt{E} + 0.05\text{ GeV}$